Experimental Neurology 312 (2019) 20–32

Contents lists available at ScienceDirect

Experimental Neurology

journal homepage: www.elsevier.com/locate/yexnr

Research paper

Vitronectin from brain pericytes promotes adult forebrain neurogenesis by stimulating CNTF

Cuihong Jia, Matthew P. Keasey, Hannah M. Malone, Chiharu Lovins, Richard R. Sante, Vlad Razskazovskiy, Theo Hagg*

Department of Biomedical Sciences, Quillen College of Medicine, East Tennessee State University, Johnson City, TN 37614, USA

ARTICLE INFO

Keywords:
Vitronectin
Focal adhesion kinase
Cytokines
gp130 signaling
Astrocyte
Neurogenesis

ABSTRACT

Vitronectin (VTN) is a glycoprotein in the blood and affects hemostasis. VTN is also present in the extracellular matrix of various organs but little is known about its function in healthy adult tissues. We show, in adult mice, that VTN is uniquely expressed by approximately half of the pericytes of subventricular zone (SVZ) where neurogenesis continues throughout life. Intracerebral VTN antibody injection or VTN knockout reduced neurogenesis as well as expression of pro-neurogenic CNTF, and anti-neurogenic LIF and IL-6. Conversely, injections of VTN, or plasma from VTN+/+, but not VTN−/− mice, increased these cytokines. VTN promoted SVZ neurogenesis when LIF and IL-6 were suppressed by co-administration of a gp130 inhibitor. Unexpectedly, VTN inhibited FAK signaling and VTN−/− mice had increased FAK signaling in the SVZ. Further, an FAK inhibitor or VTN increased CNTF expression, but not in conditional astrocytic FAK knockout mice, suggesting that VTN increases CNTF through FAK inhibition in astrocytes. These results identify a novel role of pericyte-derived VTN in the brain, where it regulates SVZ neurogenesis through co-expression of CNTF, LIF and IL-6. VTN-integrin-FAK and gp130 signaling may provide novel targets to induce neurogenesis for cell replacement therapies.

1. Introduction

Vitronectin (VTN) is a glycoprotein thought to be mainly produced by hepatocytes in the liver (Seiffert et al., 1991) and is present at high levels in the blood where it affects thrombosis, and inhibits complement-mediated cell lysis and fibrinolysis (Bergmann et al., 2009; Eberhard and Ullberg, 2002; Hallstrom et al., 2006; Preissner and Seiffert, 1998; Tomasini and Mosher, 1991; Wei et al., 1994; Zhou et al., 2003). VTN is also present at the cell surface and binds to extracellular matrix molecules in various organs (Hayman et al., 1983; Seiffert et al., 1996; van Aken et al., 1997). VTN binds integrin receptors to regulate cell attachment, proliferation, differentiation and migration in cultured cells, during development and in tissue remodeling after injury and in cancer (Milner et al., 2007; Preissner and Reuning, 2011; Preissner and Seiffert, 1998). VTN can promote inflammation by activating α5β1, αvβ5 and αvβ3 integrin (Bae et al., 2012; Dufourcq et al., 2002; Edwards et al., 2006; Milner et al., 2007). However, the role of VTN in healthy adult tissues is unclear (Leavesley et al., 2013).

VTN mRNA levels in the brain are lower compared to liver but VTN gene expression appears similar to those of hepatocytes in a subset of cells in the vicinity of brain capillaries (Seiffert et al., 1996; Seiffert et al., 1995; Seiffert et al., 1991). A recent transcriptome study identified VTN as a potential marker for adult mouse brain pericytes (He et al., 2016). The role of perivascular pericytes in the naïve brain is unclear but may include blood-brain barrier maintenance and regulation of blood flow (Hall et al., 2014; Liu et al., 2012; Winkler et al., 2011). VTN integrin receptors are expressed by astrocytes (Bello et al., 2001; Herrera-Molina et al., 2012). We have demonstrated that VTN inhibits CNTF expression in cultured astroglioma C6 cells via integrins (Keasey et al., 2013). Integrins activate intracellular signaling molecules via mediators such as focal adhesion kinase (FAK) (Giancotti and Ruoslahti, 1999; Hunter and Eckhart, 2004; Staquicini et al., 2009). Little is known about VTN functions in the healthy adult brain.

The subventricular zone (SVZ) of the adult mammalian brain, including that of humans, continues to produce new neurons (Ernst et al.,

Abbreviation: VTN, vitronectin; rhVTN, recombinant human vitronectin; CNTF, ciliary neurotrophic factor; LIF, leukemia inhibitory factor; IL-6, interleukin-6; SVZ, subventricular zone; FAK, focal adhesion kinase; ECM, extracellular matrix molecule; CD13, alanine aminopeptidase; CD31, platelet endothelial cell adhesion molecule-1; PDGFRβ, platelet derived growth factor receptor beta; DCX, doublecortin; GFAP, glial fibrillary acidic protein; FGF2, fibroblast growth factor 2; Pyk2, protein tyrosine kinase 2-beta; ILK, integrin-linked protein kinase; ERK, extracellular signal regulated kinase

* Corresponding author at: Department of Biomedical Sciences, PO Box 70582, East Tennessee State University, Johnson City, TN 37614, USA.
E-mail address: haggt1@etsu.edu (T. Hagg).

https://doi.org/10.1016/j.expneurol.2018.11.002
Received 29 May 2018; Received in revised form 17 September 2018; Accepted 5 November 2018
Available online 06 November 2018
0014-4886/

2014; Hagg, 2009; Ming and Song, 2011; Ponti et al., 2013a). In the SVZ, neural stem cells generate rapidly proliferating progenitors which differentiate into neuroblasts (Doetsch et al., 1999; Ponti et al., 2013a; Ponti et al., 2013b). The adult SVZ has a distinct vascular niche with an extensive microvasculature network and densely packed astrocytes (Shen et al., 2008; Tavazoie et al., 2008; Yang et al., 2008), which produce CNTF to promote neurogenesis (Yang et al., 2008). Astrocyte end-feet contact the extracellular matrix molecule (ECM)-rich basement membranes around endothelial cells, which regulate neurogenesis via neurotrophins and growth factors (Crouch et al., 2015; Delgado et al., 2014; Emanueli et al., 2003; Harris et al., 2017). Pericytes may contribute to this neurogenic niche with growth factors that promote progenitor proliferation and neuronal differentiation (Choi et al., 2016; Crouch et al., 2015; Trost et al., 2016). Basement membranes modulate cytokines and growth factors, perhaps thereby maintaining SVZ neurogenesis (Acevedo et al., 2015; Alvarez-Buylla and Lim, 2004; Mercier et al., 2002; Soleman et al., 2013). ECM molecules like laminin and heparan sulfate proteoglycan regulate SVZ neurogenesis and migration (Douet et al., 2012; Emsley and Hagg, 2003a; Shen et al., 2008) but nothing is known about the role of ECM VTN.

Endogenous CNTF promotes adult SVZ and hippocampal neurogenesis (Emsley and Hagg, 2003b; Yang et al., 2008), possibly through expression of FGF2 (Kang et al., 2013a), which stimulates progenitor production (Aberg et al., 2003; Ip et al., 1994; Kitchens et al., 1994; Kuhn et al., 1997; Li et al., 2008). CNTF, together with LIF and IL-6, activates the gp130 receptor signaling (Zigmond, 2011). LIF inhibits the production of progenitors by promoting stem cell self-renewal (Gregg and Weiss, 2005; Pitman et al., 2004; Shimazaki et al., 2001) in the SVZ (Bauer and Patterson, 2006). IL-6 promotes neural stem cell self-renewal (Storer et al., 2018) and counteracts progenitor proliferation and neuronal differentiation (Bowen et al., 2011; Covey et al., 2011). Inhibition of ECM molecule-integrin signaling by FAK inhibitors induces CNTF and neurogenesis (Keasey et al., 2013) but regulation of LIF and IL-6 in the SVZ is unknown.

Here, we investigated the localization and role of VTN in the regulation of CNTF, LIF, IL-6 and neurogenesis through FAK in the adult mouse SVZ. Identifying such mechanisms may help to develop pharmacological treatments to promote CNS neurogenesis for cell replacement therapies in neurological disorders.

2. Materials and methods

2.1. Animals

A total of 281 mice were used. Adult male C57BL/6 (8–10 weeks old, JAX Stock 000664), VTN transgenic mice (JAX Stock 004371) and GFAP-cre mice (B6.Cg-Tg(GFAP-cre/ERT2)505Fmv/J, JAX Stock 012849) were purchased from Jackson Laboratory. FAK-flox mice (B6;129X1-*Ptk2*^{tm1Lfr}/Mmucd, RRID:MMRRC_009967-UCD) were purchased from MMRRC at University of California at Davis. To produce experimental VTN+/+ and VTN−/− littermates, heterozygous mice were bred and genotyping was performed using tail snips and protocols provided by the suppliers. For inducible conditional astrocytic FAK knockout mice, GFAP-cre mice were bred with FAK-flox mice to generate hemizygous mice who were further backcrossed with FAK-flox mice to produce FAK-flox GFAP-cre mice (FAK$^{fl/fl}$-GFAP^{cre}) and FAK-flox (FAK$^{fl/fl}$, used as control) littermates. The Ai6 mice (B6.Cg-Gt (ROSA)26Sor $^{tm6(CAG-ZsGreen\ 1)Hze}$, JAX Stock 007906) were obtained from Dr. Diego Rodriguez-Gil's laboratory at ETSU. Homozygous Ai6 mice were bred with GFAP-cre mice to produce GFAP-cre-ZsGreen reporter (GFAP$^{cre\text{-}ZsGreen}$) and Ai6 heterozygous (used as control) mice. Tamoxifen (i.p., 100 mg/kg, twice a day for 5 days, T5648, Sigma-Aldrich) was used to induce Cre recombinase-mediated excision of LoxP sites. Experiments included both male and female mice at 8–12 weeks of age and no sex difference was detected in any of experiments. All procedures were approved by our University Committee on Animal Care and were in compliance with the NIH Guide on Care and Use of Animals.

2.2. Intrastriatal stereotactic injections

Intrastriatal injections next to the SVZ were performed as before (Kang et al., 2012). Briefly, 1 μl of test drug was injected into the middle of the striatum in one or both sides of the brain at coordinates −1 mm rostrocaudal, 1.5 mm lateral from bregma and 3.5 mm dorsoventral from the dura. The injected drugs included PBS, vehicle (1% DMSO), rabbit IgG (AP160-KC, Millipore), rabbit anti- mouse VTN antibody (8.2 μg/μl, Ab62769, Abcam, RRID:AB_956454), recombinant human VTN (rhVTN, 1 μg/μl, Sigma, SRP3186), rhVTN + SC144 (3.6 ng/μl, #4963) or FAK14 (2.4 μg/μl, Tocris Bioscience, #3414). The SVZ was collected 3 or 24 h later and stored at −80 degree for mRNA and protein extraction. SC144 has been identified as a selective gp130 inhibitor by directly binding to the gp130 receptor, causing its Ser782 phosphorylation and deglycosylation, and subsequent degradation. This reduces downstream intracellular activation of STAT3 and Akt by the gp130 ligands, IL-6 and LIF (Grande et al., 2016; Xu et al., 2013). However, SC144 has no effect on activation of STAT3 and Akt caused by non-gp130 cytokines, interferon γ and stromal cell-derived factor 1α, and platelet-derived growth factor (Xu et al., 2013), suggesting it is selective for gp130 over other types of receptors tested. Those investigators suggested that it can bind to and stabilize IL-24, resulting in cell cycle arrest and apoptosis of cancer cells (Xu et al., 2013). However, IL-24 is undetectable by in situ hybridization in the brain, including the SVZ (Allen Brain Atlas), and SC144 alone did not affect SVZ cell proliferation or neuroblast numbers in mice (Fig. 5). To label proliferating cells in naïve mice or following intrastriatal injections, mice were injected with BrdU (i.p.) at 50 mg/kg twice a day for 3 days and perfused with ice-cold PBS and 4% PFA 2 h after last injection. In the SC144 experiment they were injected with BrdU at 144 mg/kg at 21, 24 and 27 h and perfused at 48 h.

2.3. Immunohistochemistry

Coronal sections (30 μm) through the brain, and sections through the heart and liver were stained with the rabbit anti-mouse vitronectin antibody (1:1000, ab62769, Abcam) alone or together with one of the following: goat anti-DCX (1:500, SC-8066, Santa Cruz, RRID:AB_2088494), mouse anti-GFAP (1:1000, MAB3402, Millipore, RRID:AB_94844), rat anti-CD31 (1:500, #550274, BD Pharmingen, RRID:AB_393571), Goat anti-CD13 (1:50, AF2335, R&D Systems, RRID:AB_2227288) or rat anti-PDGFRβ (1:500, #14-1402-82, Invitrogen, RRID:AB_467493) antibody, and followed by Alex Fluor 488-conjugated donkey anti-rabbit and Alex Fluor 594-conjugated donkey anti-goat, mouse or rat secondary antibody (all from Invitrogen) to visualize the positive immunofluorescent staining. The nuclei were counterstained with Hoechst. The specificity of the VTN antibody was validated by detecting no staining in tissue from VTN−/− mice stained with primary and secondary antibody, and wildtype tissue stained with purified IgG instead of primary antibody or staining with primary or secondary antibody alone. We also tested a number of other commercially available VTN antibodies. R&D MAB38751 (RRID:AB_2216439) and Santa Cruz SC74484 (RRID:AB_1131298) did not show any staining in brain tissue. Abcam ab28023 (RRID:AB_778869), Abcam ab45139 (RRID:AB_778872), and Molecular Innovations ASMVN, lightly stained SVZ processes in both VTN+/+ and VTN−/− brain tissue sections. ASMVN also revealed small striatal neurons in both genotypes. Only the Abcam ab62769 antibody (RRID:AB_956454) showed specific staining (in pericytes) and revealed no immunoreactivity in KO tissue, validating it as specific. Finally, to confirm cre activity in the cre-lox mice, we used rabbit anti-ZsGreen 1 (1:1000, #632474, Clontech Laboratories, RRID:AB_2491179) antibody followed by donkey anti-rabbit secondary conjugated to Alex Fluor 488 to visualized ZsGreen 1

protein expression in brain sections.

2.4. Unbiased and stereological analysis for BrdU-positive nuclei

Every sixth 30 μm thick coronal section through the SVZ along rostrocaudal axis (total six sections/brain) were stained with BrdU using rat anti-BrdU antibody (1:1000, ab6326, Abcam RRID:AB_305426) or stained with BrdU and DCX using rat anti-BrdU antibody and goat anti-DCX antibody as described previously (Jia and Hegg, 2015). Unbiased stereological analysis of BrdU-positive cells in the SVZ was performed using a motorized Leica DMIRE2 microscope and an optical fractionator stereological method (Stereologer, System Planning and Analysis, Alexandria, VA) by researchers blinded to the treatment (Kang et al., 2013a). The numbers of DCX-positive and DCX-BrdU co-labeled neuroblasts in the most populated dorsolateral part of SVZ (640 μm × 480 μm) in every sixth section through SVZ were also counted by researchers blinded to the treatments. The DCX-positive cells were defined by their DCX-positive cytoplasm surrounding Hoechst-labeled or BrdU-labeled nuclei. The quantification of VTN-positive cells in the dorsolateral SVZ and medial striatum, and PDGFRβ-VTN co-labeled or CD13-VTN co-labeled cells in the dorsolateral SVZ was performed in the z-stacks of confocal pictures with an area of 465 μm × 465 μm (3 sections each mouse and two images including left and right side each section).

2.5. Protein and mRNA analyses

The CNTF, pFAK, FAK, pPyk2, Pyk2, pILK, ILK, pERK, ERK and α-tubulin proteins in the SVZ were detected with western blotting as described previously (Keasey et al., 2013) with the following antibodies: CNTF (1:500, MAB338, RRID:AB_2083064), pFAK (1:1000, #3283, RRID:AB_10327658), FAK (1:1000, #3285,RRID:AB_2269034), pPyk2 (1:1000, #3291,RRID:AB_2300530), Pyk2 antibody (1:1000, #3480,RRID:AB_2174093), pILK (1:1000, AB1076,RRID:AB_10807157), ILK (1:1000, 04-1149,RRID:AB_1977290), pERK (1:2000, #9106,RRID:AB_331768), ERK (1:2000, #9102,RRID:AB_330744) and α-tubulin (1:2000, #2125,RRID:AB_2619646). The levels of pFAK and α-tubulin were also quantitatively measured by WES Quantitative Capillary Electrophoresis according to the manufacturer's protocol (ProteinSimple, PS-MK01) as described previously (Keasey et al., 2018; Visavadiya et al., 2016). Briefly, tissue homogenates (1 μg protein, 0.2 μg/μl) mixed with fluorescent molecular weight markers were loaded into 24 single designated wells followed by antibody diluent, mixture primary antibodies (1:25, pFAK and 1:200, α tubulin, in antibody diluent), anti-rabbit HRP-conjugated secondary antibody and luminol-peroxide mixture and wash buffer loaded into different wells aligned with tissue samples. Plates were loaded into the automated ProteinSimple Wes for electrophoresis and fluorescence imaged in real time by a CCD camera. Data was expressed as peak intensity or synthetic bands. The quantification was performed by normalizing the area under pFAK peak to α-tubulin loading control in each capillary and then the values were normalized to the average of PBS. IL-6 and LIF protein levels in the SVZ were measured using ELISA according to manufacturer's protocols (R & D system, IL-6, M6000B, LIF, MLF00). Briefly, 25 μg total protein from SVZ tissue homogenate in 50 μl was run together with standard curve in duplications.

The mRNA levels of CNTF, LIF and IL-6 in the SVZ were measured by RT-qPCR as described previously (Kang et al., 2013a). To detect differences in the low basal levels of CNTF, LIF and IL-6 in the SVZ between VTN+/+ and VTN−/− mice we used semi-nested RT-qPCR following a previously described method (Pasternak et al., 2008) with modifications. Briefly, cDNA was reverse transcribed from 20 ng SVZ RNA was PCR amplified for 5, 10, 15 or 20 cycles to test the optimal cycle numbers for pre-amplification. Primers for CNTF (Mm00446373_m1), IL-6 (Mm00446190_m1) and LIF (Mm00434762_g1) were from Life Technologies. We chose 20 cycles since the amplification curve displayed an exponential phase for all genes at 20 cycles. PCR conditions for pre-amplification were 20 s at 95 °C (ramp rate 1.9 °C/s) for initial denaturation and then 20 cycles of 1 s at 95 °C (1.9 °C/s ramp rate) followed by 20 s at 60 °C (ramp rate 1.6 °C/s) for amplification. The pre-amplification of cDNA was performed in duplicates on a QuantStudio 6 Flex (Applied Biosystems) in total 5 μl reaction per well of 384 well plate. The PCR products from pre-amplification were pooled for each sample and 1 μl of pre-amplification product was used for semi-nested, real-time qPCR as described previously (Keasey et al., 2018).

2.6. Statistical analyses

Statistical analyses were performed using graphpad Prism (version 7). A value of $p < 0.05$ was considered to be statistically significant. A one-way ANOVA with Bonferroni post hoc multiple comparisons was applied when there were three or more groups with testing for one factor. A two-way ANOVA with post hoc Tukey multiple comparisons was used when the groups were four or more and there were two factors to be tested, such as genotypes and treatments. If only two groups were compared, a Student's *t*-test was used.

3. Results

3.1. VTN protein is uniquely expressed in the pericytes of the adult SVZ

In the adult mouse SVZ (Fig. 1A,E,F) and striatum (Fig. 1B,D), VTN immunostaining was present in cells located alongside and very close to blood vessels. Their processes often appeared to surround the entire vessel (insets in Fig. 1B). Specificity of the antibody was shown by the lack of any staining in the SVZ of VTN−/− mice (Fig. 1C). The number of VTN-positive cells in the dorsolateral part of SVZ was more than double that seen in the striatum (215 ± 56 vs. 82 ± 7 per mm^2, $p = 0.039$, student's *t*-test, $n = 3$ mice each). SVZ VTN-positive cells were apposed to microvessels, especially at points of bifurcations, which were particularly noticeable in the striatum (Fig. 1D) where the microvascular network is not as dense as in the SVZ. We observed the same staining patterns in the cerebral cortex (not shown). VTN expression did not co-localize with vascular endothelial cells stained for CD31 (Fig. 1E,F) but the VTN-positive cells appeared to be in direct contact with the endothelial cells. Neuroblasts travel along microvessels but VTN did not co-localize with the neuroblast marker doublecortin (Fig. 1G–I). A search of VTN mRNA expression in the Allen mouse brain atlas (http://mouse.brain-map.org) identified a peri-vascular pattern of cells resembling that of PDGFRβ mRNA in the dorsolateral SVZ and elsewhere in the brain. PDGFRβ has been used as a pericyte marker (Sato et al., 2016; Sweeney et al., 2016). VTN was clearly co-localized with PDGFRβ (Fig. 2A-C,J) and with CD13 (Fig. 2D-F,K), which is also expressed by pericytes (Sato et al., 2016; Sweeney et al., 2016). These data indicate that VTN is uniquely expressed in pericytes of adult mouse SVZ. Not all PDGFRβ or CD13-positive pericytes had overt VTN staining. In the SVZ, 53 ± 6% of PDGFRβ-positive cells were VTN-positive and 40 ± 7% of CD13-positive cells expressed VTN. These data suggest that a substantial sub-population of pericytes produce most of the VTN in the brain. Interestingly, we observed that VTN-positive cells often were in direct contact with GFAP-positive astrocyte processes, which sometimes enveloped the pericyte cell body (Fig. 2G–I,L,M). This raises the possibility that pericytes can affect the function of astrocytes in the SVZ through VTN-mediated integrin signaling.

Given the abundant expression of VTN in the liver, we also investigated the localization of VTN. Immunostaining was present around the portal area and the central veins, and along the sinusoids between them (Suppl. Fig. 1A,B). VTN staining was most prominent in the periportal area followed by that around the peri-central vein. Surprisingly, the hepatocytes had little or no positive staining. VTN-

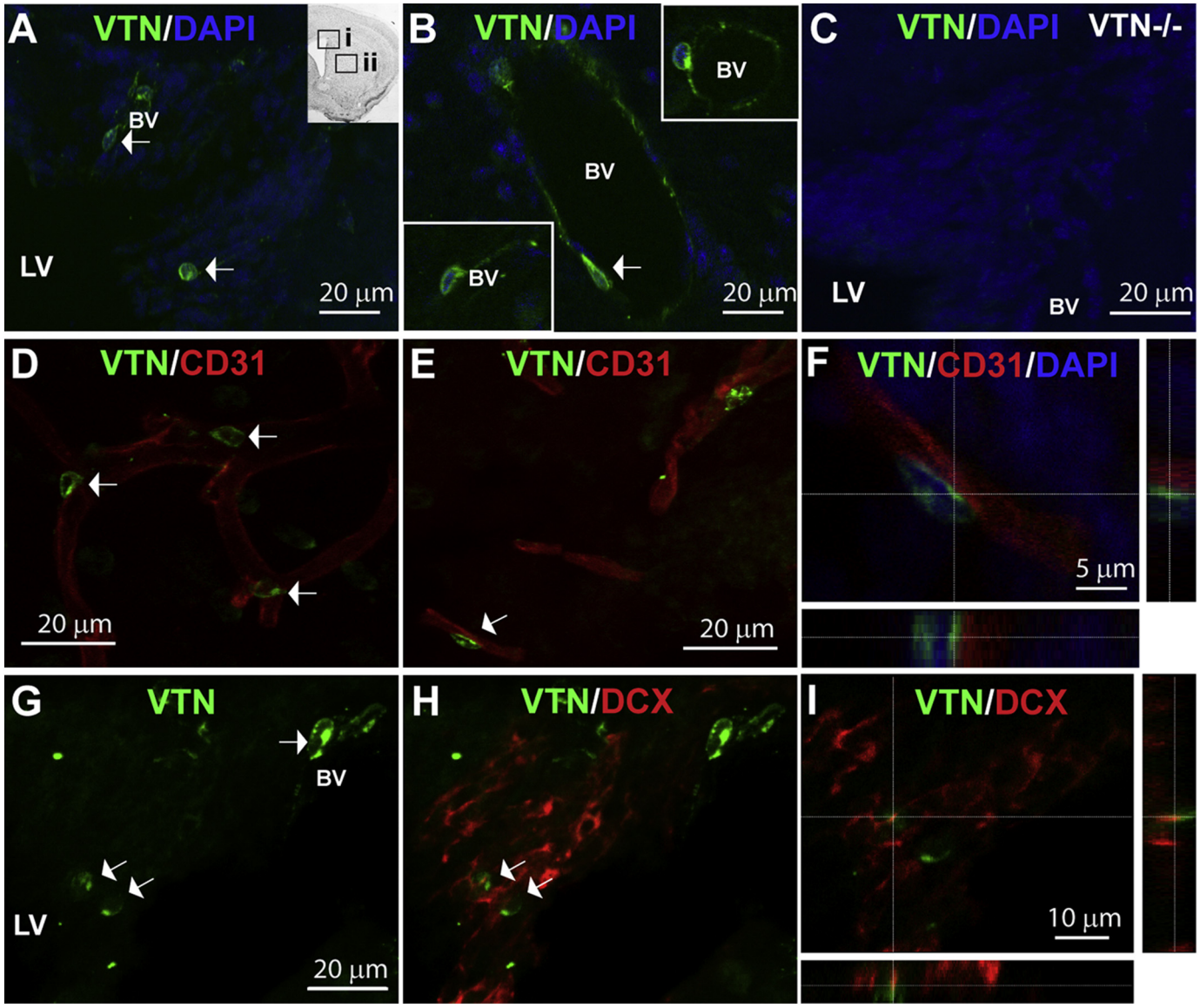

Fig. 1. VTN is expressed in perivascular cells of the adult mouse brain. Confocal images show VTN immunostaining in the SVZ (A) and striatum (B). Arrows indicate examples of VTN-positive cells. Nuclei were stained with DAPI (blue). Inset in (A) shows the locations of SVZ (i) and striatum (ii) images in a coronal section. Two insets in (B) show VTN-positive cells around two microvessels in the striatum. LV = lateral ventricular, BV = blood vessel. Scale bars are as indicated. C) No VTN-positive staining was present in VTN−/− mice, validating the specificity of the antibody. D) VTN-positive cells were located at bifurcation points of striatal blood vessels identified by the endothelial marker CD31. E) VTN-positive cells in the SVZ are tightly apposed to endothelial cells as shown by lack of co-localization with CD31 in (F). G–I) VTN-positive cells in the SVZ were not co-localized with doublecortin (DCX)-positive neuroblasts. The VTN-positive cells indicated by arrows in (G,H) are shown in one 1 μm thick section of a confocal z-stack (I). (For interpretation of the references to colour in this figure legend, the reader is referred to the web version of this article.)

positive cells were located on the abluminal side of the vascular endothelial cells (Suppl. Fig. 1a,b,b′), and in the space of Disse, the perisinusoidal space between sinusoidal endothelial cells and hepatic cells (Suppl. Fig. 1b″). VTN was highly co-localized with CD13 (Suppl. Fig. 1C–E,e, e′), indicating that VTN is expressed in the liver pericytes which are liver-specific mesenchymal cells also known as stellate cells (Di Matteo et al., 2011; Hellerbrand, 2013; Huang et al., 2016). VTN has also been found in the heart, and VTN staining was located around blood vessels (Suppl. Fig. 1F–H) and no staining was observed in cardiomyocytes. VTN was not co-localized with the endothelial cell marker CD31 (Suppl. Fig. 1h), but co-localized with CD13 (Suppl. Fig. 1I–K,k), indicating that pericytes produce VTN in the heart.

3.2. VTN promotes CNTF, IL-6 and LIF expression and SVZ neurogenesis

To determine whether pericyte VTN affects expression of cytokines that regulate neurogenesis, the same validated VTN antibody was injected into the striatum next to the SVZ of C57BL/6 mice. After 24 h, the antibody caused a reduction in CNTF (−46%), IL-6 (−33%) and LIF (−19%) mRNA expression in the SVZ compared to the isotype control IgG (Fig. 3A). Moreover, naive adult VTN−/− mice had reduced expression of CNTF (−26%), IL-6 (−31%) and LIF (−38%) mRNA in the SVZ compared to naïve VTN+/+ littermate mice (Fig. 3B). In concert, cell proliferation and SVZ neurogenesis in the SVZ was reduced in VTN−/− mice as measured by the numbers of cells labeled with BrdU (Fig. 3C,D, −18%), the neuroblasts labeled by DCX (Fig. 3E,F, −24%) as well as co-labeled with BrdU and DCX (Fig. 3G,H, −63%).

As a gain-of-function experiment, we injected rhVTN protein in the

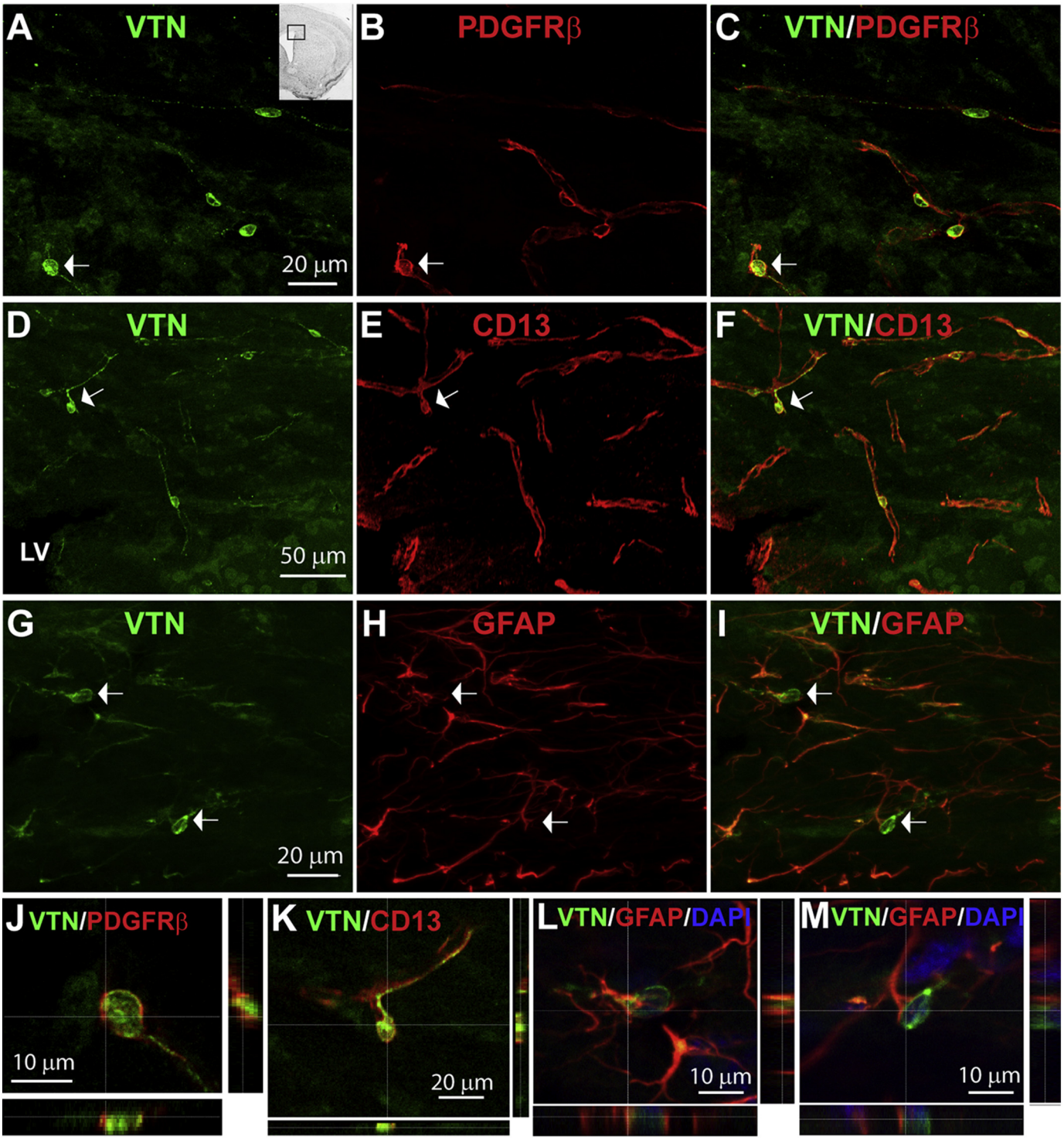

Fig. 2. VTN is uniquely expressed in pericytes of the adult mouse SVZ. VTN was co-localized with the pericyte markers, PDGFRβ A–C) and CD13 D–F) as shown in confocal images of the SVZ. The arrows indicated in (C,F) are shown at higher magnification in J) and K). VTN-positive cells were closely apposed to GFAP-positive astrocytes G–I). The cells indicated by the arrows are shown at higher magnification in L) and M). The inset in (A) shows the location of the SVZ images in this fig. LV = lateral ventricle. Scale bars are as indicated.

striatum next to the SVZ. We used wildtype VTN+/+ mice, but also VTN−/− littermates, to circumvent any potential confounding effects of blood VTN leaking into the injection site. At 24 h, in both VTN+/+ and VTN−/− mice, rhVTN substantially increased mRNA levels of CNTF (Fig. 4A), IL-6 (Fig. 4B), and LIF (Fig. 4C) compared to control PBS injections. The expression levels in PBS- or rhVTN-injected VTN +/+ and VTN−/− mice were comparable and not significantly different, ruling out the potential contribution of leaked blood VTN. This seems to be in apparent contradiction to reduced cytokine expression in the SVZ of naïve VTN−/− mice (Fig. 3B). Previously, intrastriatal injection of PBS slightly increased IL-6 and LIF in the SVZ (Jia et al., 2018), raising the possibility that VTN−/− mice are more sensitive to intrastriatal injections than their wild type littermates. Intrastriatal injection of rhVTN also increased CNTF (Fig. 4D,E), IL-6

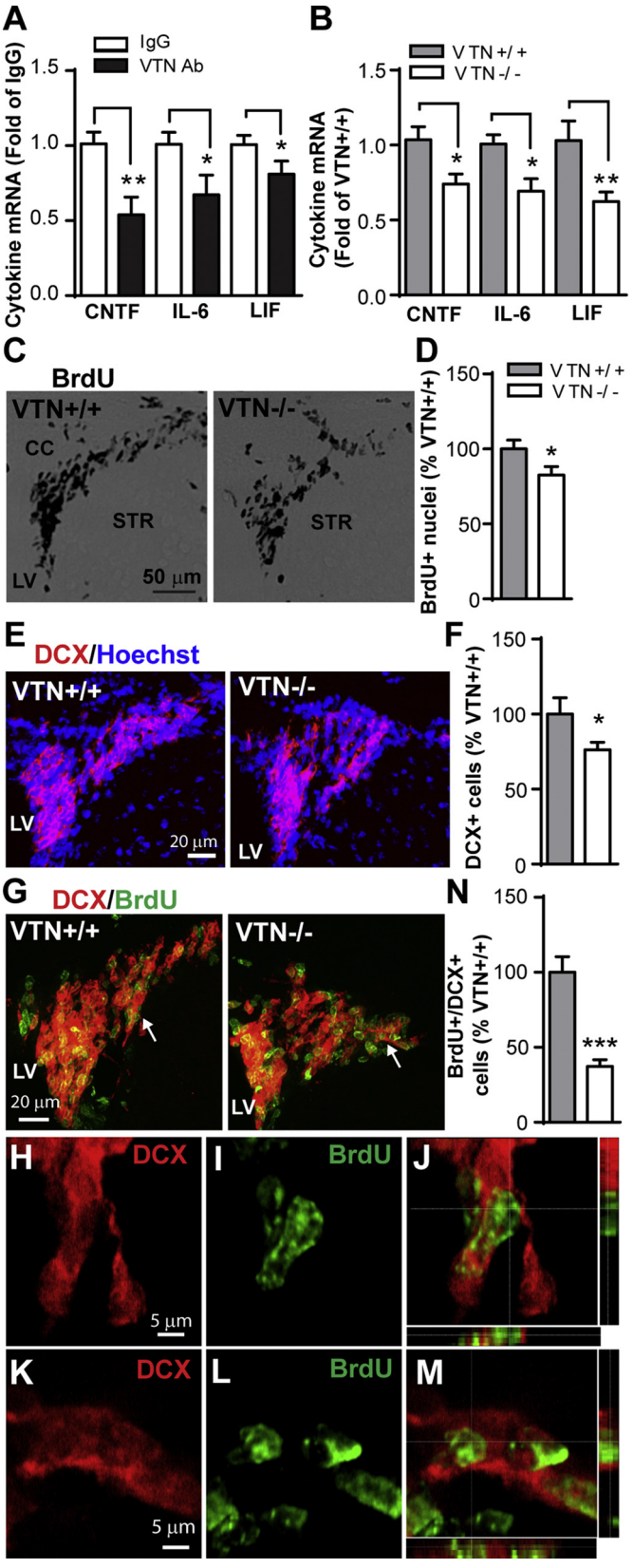

Fig. 3. VTN inhibition or deletion reduces expression of CNTF, LIF and IL-6 and cell proliferation in the SVZ. A) Intrastriatal injection of a VTN antibody reduced CNTF, IL-6 and LIF mRNA in the neighboring SVZ of C57BL/6 mice at 24 h later. Data are mean + SEM and calculated as fold change of IgG ($n = 5$ and 5 mice, *p < 0.05, **p < 0.01, Student's *t*-test). B) VTN−/− mice had lower mRNA levels of CNTF, IL-6 and LIF in the SVZ compared to VTN+/+ mice as measured by semi-nested RT-qPCR. Data are mean + SEM and calculated as fold change of the VTN+/+ mice (n = 5 and 9 mice, * p < 0.05, ** p < 0.01, Student's *t*-test). C) Representative images of BrdU immunostaining in coronal sections through the SVZ of adult VTN+/+ and VTN−/− mice following 3 daily BrdU injections show a decrease in proliferation in the SVZ of VTN−/− mice. LV = lateral ventricle, STR = striatum and CC = corpus callosum. D) Unbiased stereological counting of BrdU-positive nuclei in the SVZ confirmed that VTN−/− mice had ~18% less cell proliferation than VTN+/+ mice (n = 4 and 5 mice, * p < 0.05, student's *t*-test). E) Representative images of DCX (red) immunostaining in the dorsolateral SVZ of adult mice show a decrease in neuroblasts in the SVZ of VTN−/− compared to VTN+/+ mice. Nuclei were stained with Hoechst (blue). F) Quantification of DCX-positive cells in the SVZ confirmed that VTN−/− mice had ~24% fewer neuroblasts than VTN+/+ mice (n = 4 and 5 mice, * p < 0.05, student's *t*-test). G) Representative images of DCX (red) and BrdU (green) immunostaining in the dorsolateral SVZ show a decrease in BrdU-labeled neuroblasts in the SVZ of VTN−/− mice. High magnification of BrdU-DCX co-labeled cells (arrows in G) in VTN+/+ H–J) and VTN−/− K–M) mice show examples of counted cells. N) Quantification of BrdU–DCX co-labeled cells in the SVZ confirmed that VTN−/− mice had ~63% less neurogenesis than VTN+/+ mice (n = 4 and 5 mice, ***p < 0.001, student's *t*-test). (For interpretation of the references to colour in this figure legend, the reader is referred to the web version of this article.)

(Fig. 4F) and LIF (Fig. 4G) protein expression in the SVZ, as measured by western blot and ELISA. The levels of VTN-induced protein expression were not different between the two genotypes. This suggests that the knockout mice did not undergo developmental adaptive compensation, such as expression of integrins which bind to VTN to regulate these cytokines. This was confirmed by similar mRNA levels of the αv, β3 and β5 integrin receptor subunits in the SVZ of VTN+/+ and VTN−/− mice (data not shown).

Blood contains very high concentrations of VTN (around 300 µg/ml), representing ~1% of plasma protein (Hogasen et al., 1993; Seiffert et al., 1991; Shaffer et al., 1984). By comparing the effects of plasma from VTN+/+ and VTN−/− mice we could test whether native endogenous mouse VTN had similar activities as the rhVTN and the unique role of VTN among other plasma proteins or factors that might affect cytokine production and neurogenesis (Lin et al., 2018). We again also used VTN−/− mice to rule out effects of leaked plasma due to the injection. At 24 h after intrastriatal injection, VTN+/+ plasma substantially increased SVZ CNTF (Fig. 4H), IL-6 (Fig. 4I) and LIF (Fig. 4J) expression in both VTN+/+ and VTN−/− mice. Strikingly, VTN−/− plasma did not significantly alter expression of these cytokines. These data suggest that VTN is a major and possibly unique ECM protein regulating CNTF, LIF and IL-6 in the brain.

3.3. Exogenous VTN increases neurogenesis when IL-6 and LIF are reduced by gp130 inhibition

Previously, we found that intrastriatal injection of IL-6 stimulates CNTF, LIF and IL-6 in adult mouse SVZ (Kang et al., 2013b) which can bind to their common gp130 receptor (Zigmond, 2012). To test whether VTN-stimulated CNTF, LIF or IL-6 expression induces a gp130-mediated feedforward mechanism, we injected rhVTN with or without the gp130 inhibitor, SC144, into striatum next to the SVZ of C57BL/6 mice. Consistent with the results in Fig. 4, at 24 h, VTN increased all three cytokines in the SVZ (Fig. 5A–C). SC144 alone did not alter the basal expression levels. Co-injection of SC144 with rhVTN did not alter VTN-induced CNTF (Fig. 5A) but reduced IL-6 (Fig. 5B) and LIF (Fig. 5C) by 40–50%. This suggests that VTN-induced LIF and IL-6 involve a gp130-mediated feed-forward mechanism, and that blocking it shifts the balance of cytokine expression in favor of pro-neurogenic CNTF. Expression of FGF2, which promotes formation of progenitors (Aberg et al., 2003; Kuhn et al., 1997; Li et al., 2008), was increased in the SVZ by

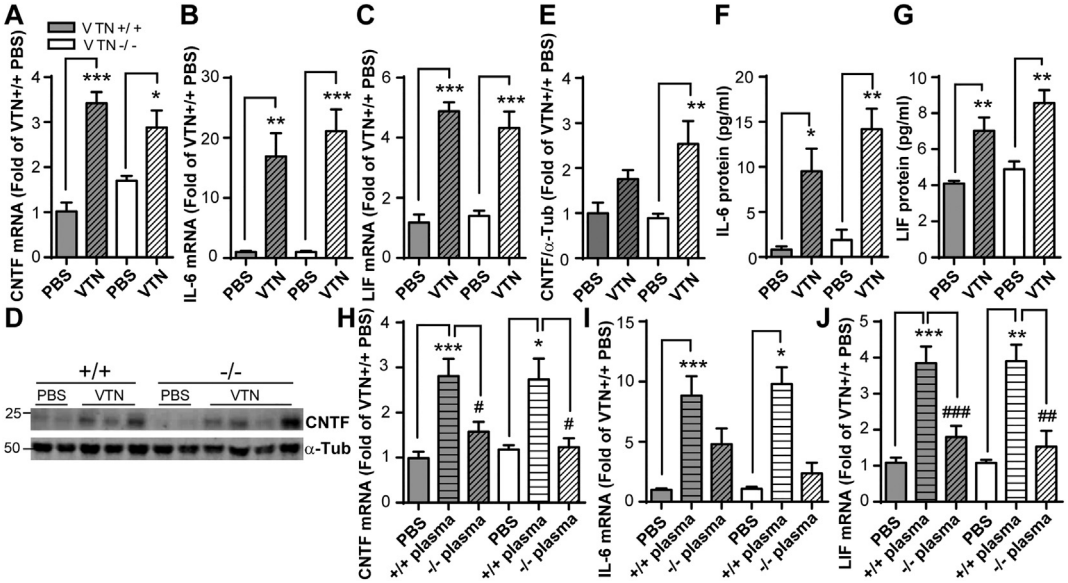

Fig. 4. VTN injection increases CNTF, LIF and IL6 expression in the SVZ. Intrastriatal injection of rhVTN increased A) CNTF, B) Il-6 and C) LIF mRNA in the SVZ of both VTN+/+ and VTN−/− mice at 24 h later. Data are mean + SEM and calculated as fold change of the group average of the PBS VTN+/+ mice. VTN also increased CNTF protein levels in the same mice, as shown by western blot (D) and densitometry quantification (E). IL-6 F) and LIF G) protein levels were increased in the same mice as shown by ELISA (n = 5, 5, 4 and 5 per group. *p < 0.05, **p < 0.01, ***p < 0.001, Two-way ANOVA followed by post hoc Tukey multiple comparison test). In separate mice, intrastriatal injection of plasma collected from VTN+/+, but not VTN−/−, mice increased CNTF (H), IL-6 (I) and LIF (J) mRNA expression in the SVZ of VTN+/+ and VTN−/− mice at 24 h. Data are mean + SEM and calculated as fold change of the group average of the PBS VTN+/+ mice (*n* = 8, 7 and 8 VTN+/+ mice/group and n = 5, 3 and 6 VTN−/− mice/group. * or # p < 0.05, ** or ## p < 0.01, *** or ###p < 0.001, Two-way ANOVA followed by post hoc Tukey multiple comparison test).

both VTN and VTN + SC144 (Fig. 5D). However, only VTN + SC144 increased the expression of EGFR (Fig. 5E), a marker for these progenitors (Doetsch et al., 2002). Next, SVZ neurogenesis was quantified at 48 h after the intrastriatal injection, with BrdU being injected i.p. at 21, 24 and 27 h. Intrastriatal injection of VTN + SC144, but not VTN or SC144 alone, substantially increased the number of BrdU-positive nuclei (Fig. 5F,G), DCX-positive neuroblasts (Fig. 5H,I) and BrdU-DCX co-labeled neuroblasts (Fig. 5J,K) in the SVZ. These data suggest that VTN rapidly increases neurogenesis when the balance of cytokine expression favors CNTF-induced progenitor proliferation, perhaps also including effects on FGF2 expression, as we have suggested before (Kang et al., 2013a).

3.4. VTN induces CNTF, LIF and IL-6 via FAK inhibition

VTN binds to integrins which are well-known to activate downstream FAK signaling. Wildtype VTN+/+ mice were injected with PBS or rhVTN and SVZ tissue collected at 3 h. Surprisingly, the levels of phospho-FAK (pFAK) appeared to be decreased by injected VTN in most mice compared to PBS (Fig. 6A). Quantitative capillary western analysis showed that VTN inhibited FAK phosphorylation by ~37% in the SVZ (Fig. 6B–D). In C57BL/6 mice, intrastriatal injection of rhVTN also led to a reduction in pFAK in the SVZ compared to PBS at 3 h (Fig. 6E). Activation of another major signaling molecule downstream of integrins, Pyk2 (Mitra et al., 2005; Sulzmaier et al., 2014), was also inhibited in the SVZ of the VTN+/+ mice by intrastriatal injection of rhVTN (Fig. 6F). Conversely, activation of downstream ILK (Widmaier et al., 2012) was increased in the SVZ 3 h after intrastriatal injection of rhVTN (Fig. 6G). VTN also reduced the level of pERK, which is downstream of FAK, in the SVZ at 3 h (Fig. 6H). At 24 h, pFAK was not different between intrastriatal rhVTN and PBS injected mice (data not shown). Consistent with VTN-inhibited pFAK, the levels of pFAK in the SVZ of VTN−/− mice were significantly increased compared to those in VTN+/+ mice (Fig. 6I,J), suggesting the decreases of CNTF, LIF and IL-6 in VTN−/− mice may be due to higher levels of pFAK.

Next, we determined whether astrocytes, which produce CNTF, are involved in FAK inhibitor-and VTN-induced expression of CNTF, IL-6 and LIF in the SVZ. We cross-bred existing mouse lines to produce tamoxifen-inducible conditional deletion of FAK in adult GFAP-positive astrocytes (Sup. Fig. 2A). Successful cre-mediated recombination was confirmed by PCR of DNA from the SVZ of tamoxifen-treated $FAK^{fl/fl}$-$GFAP^{Cre}$ mice (data not shown). Tamoxifen-induced Cre activity in astrocytes was shown by co-localization of ZsGreen protein with GFAP in tamoxifen-treated $GFAP^{cre\text{-}ZsGreen}$ reporter mice (Sup. Fig. 2B–E). Two weeks after the last tamoxifen injection the mice received intrastriatal injections and were analyzed 24 h later. CNTF expression in the SVZ was increased in the PBS-injected $FAK^{fl/fl}$-$GFAP^{Cre}$ mice (Fig. 6K,N) compared to PBS-injected control $FAK^{fl/fl}$ mice, suggesting that knockout of FAK in astrocytes increases CNTF expression. As expected, the FAK inhibitor FAK14 or VTN increased CNTF in $FAK^{fl/fl}$ control but not in the $FAK^{fl/fl}$-$GFAP^{Cre}$ mice (Fig. 6K,N), indicating that FAK14 or VTN acts entirely by inhibiting astrocytic FAK. The levels of IL-6 were not affected by the conditional FAK knockout in the astrocytes and FAK14- or VTN-induced IL-6 expression was not different between $FAK^{fl/fl}$ and $FAK^{fl/fl}$-$GFAP^{Cre}$ mice (Fig. 6L,O), suggesting that FAK14- or VTN-induced IL-6 is produced by other cells. LIF expression was not affected by the conditional FAK knockout (Fig. 6M,P), but FAK14-induced LIF expression was lower in $FAK^{fl/fl}$-$GFAP^{Cre}$ than the control $FAK^{fl/fl}$ mice (Fig. 6 M), suggesting that astrocyte FAK mediates some of the FAK14 effects on LIF expression. The levels of VTN-induced LIF expression were comparable in control $FAK^{fl/fl}$ and $FAK^{fl/fl}$-$GFAP^{Cre}$ mice (Fig. 6P).

3.5. Astrocyte-specific knockout of FAK increases SVZ neurogenesis

In order to test whether astrocyte-specific knockout of FAK increases SVZ neurogenesis, we quantified the numbers of BrdU-positive nuclei in the SVZ of $FAK^{fl/fl}$ and $FAK^{fl/fl}$-$GFAP^{Cre}$ mice following 3 days of BrdU injection using unbiased stereology. Compared to $FAK^{fl/fl}$ mice, $FAK^{fl/fl}$-$GFAP^{Cre}$ mice had a 27% increase in BrdU-positive nuclei in the SVZ (Fig. 7A,B). We also measured the numbers of BrdU-DCX- co-labeled neuroblasts in the dorsolateral SVZ to confirm that increased

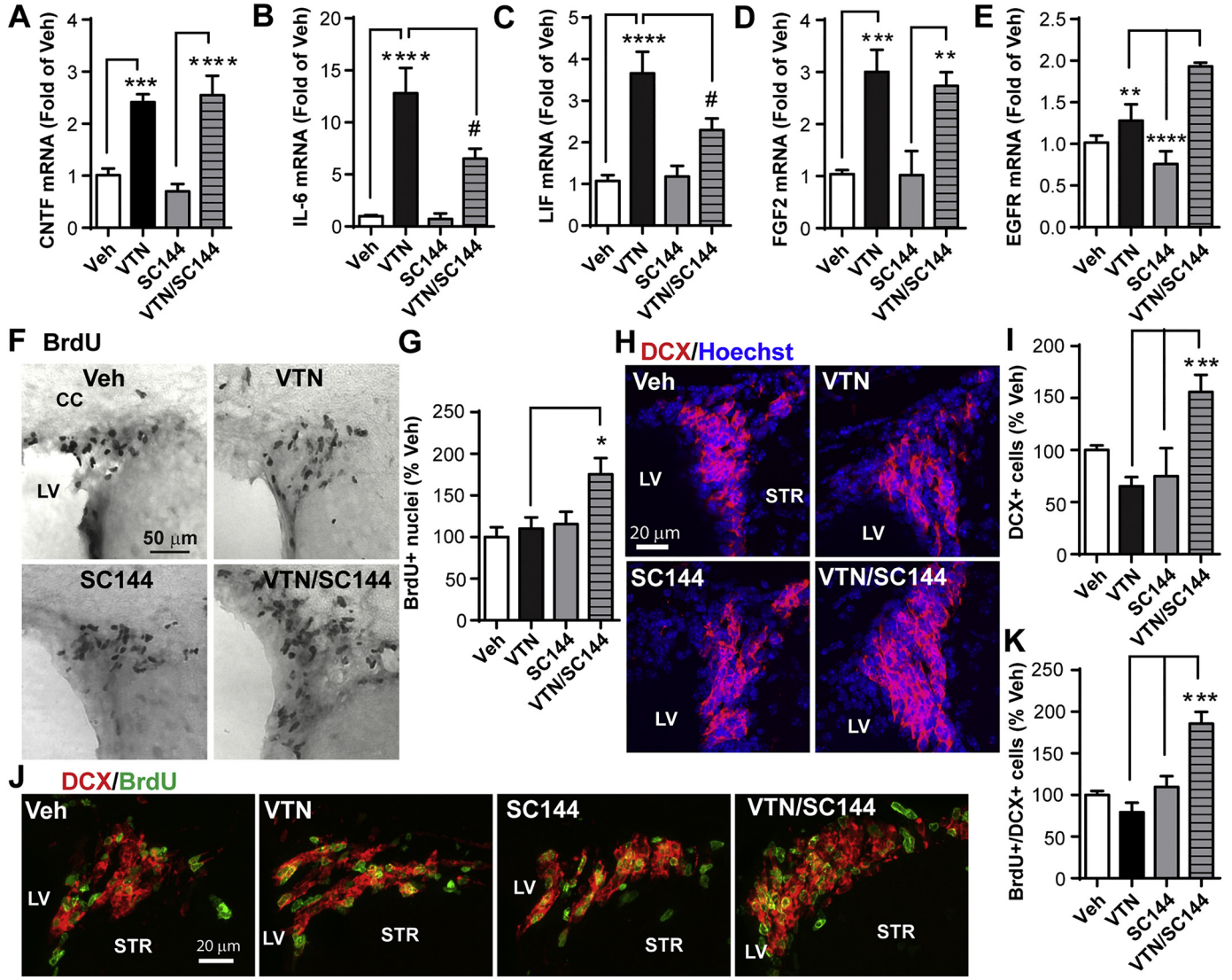

Fig. 5. VTN increases SVZ neurogenesis when LIF and IL-6 expression is inhibited by a gp130 inhibitor. Intrastriatal injection of both rhVTN and the gp130 receptor inhibitor, SC144, did not affect A) VTN-induced CNTF expression in the SVZ of C57BL/6 mice, but suppressed VTN-induced B) IL-6 and C) LIF. Data are mean + SEM and calculated as a fold change over the vehicle (Veh, 1% DMSO) group average (n = 9, 7, 5 and 6 mice/group. ***p < 0.001, ****p < 0.0001, Two-way ANOVA followed by post hoc Tukey multiple comparison test). D) VTN increased FGF2, known to promote progenitor formation, but not the progenitor marker EGFR (E), but increased both in the presence of SC144, as shown in the same SVZ samples as (A-C). F) Representative images of BrdU immunostaining in coronal sections through the dorsolateral SVZ of adult C57BL/6 mice at 48 h following intrastriatal injection show an increase in proliferation in the VTN plus SC144 (VTN/SC144) group compared to the others. LV = lateral ventricle and CC = corpus callosum. G) Unbiased stereological counts of BrdU-positive nuclei in the SVZ confirmed that co-administration of SC144 enables VTN to induce proliferation. Data are mean + SEM, with the vehicle group set at 100% (n = 6, 5, 5 and 5 mice/group. *p < 0.05, Two-way ANOVA followed by post hoc Tukey multiple comparison test). H) Representative confocal images of DCX (red) immunostaining in coronal sections through SVZ of the same groups of adult C57BL/6 mice. Nuclei were stained with Hoechst (blue). I) Cell counts in the SVZ confirmed that VTN/SC144 increased the number of DCX-positive neuroblasts (*** p < 0.001, Two-way ANOVA followed by post hoc Tukey multiple comparison test). J) Representative confocal images of DCX (red) and BrdU (green) immunostaining in the dorsolateral SVZ of the same adult C57BL/6 mice. K) Quantification of BrdU–DCX co-labeled cells in the SVZ confirmed that VTN/SC144 increased neurogenesis (***p < 0.001, Two-way ANOVA followed by post hoc Tukey multiple comparison test). (For interpretation of the references to colour in this figure legend, the reader is referred to the web version of this article.)

proliferation (BrdU) leads to more neurogenesis. Compared to $FAK^{fl/fl}$ mice, $FAK^{fl/fl}$-$GFAP^{Cre}$ mice had a 2-fold increase in BrdU-DCX-positive cells (Fig. 7C,D). The mRNA expression levels of VTN in the SVZ of $FAK^{fl/fl}$-$GFAP^{Cre}$ mice were not different from the $FAK^{fl/fl}$ mice (0.93 ± 0.08 vs. 1.0 ± 0.03, calculated as a fold of $FAK^{fl/fl}$, $n = 4$ and 7 mice, p = 0.21, Student's *t*-test), confirming that the effects of the FAK deletion were not due to changes in the endogenous VTN expression. These data indicate that knockout of FAK in the astrocytes increases SVZ neurogenesis, possibly through CNTF.

4. Discussion

We identified VTN as being uniquely expressed by brain pericytes and as a novel regulator of normal adult forebrain neurogenesis through cytokine expression and highlight the role of microvascular pericytes. VTN−/− mice have a subtle phenotype, including an increased rate of thrombosis after vascular injury and reduced angiogenesis after tissue injury (Eitzman et al., 2000; Jang et al., 2000). In the cerebellum of VTN−/− mice, the granule cell precursors have dysfunctional initial differentiation during development (Hashimoto et al., 2016). Little was known about the role of VTN in healthy adult

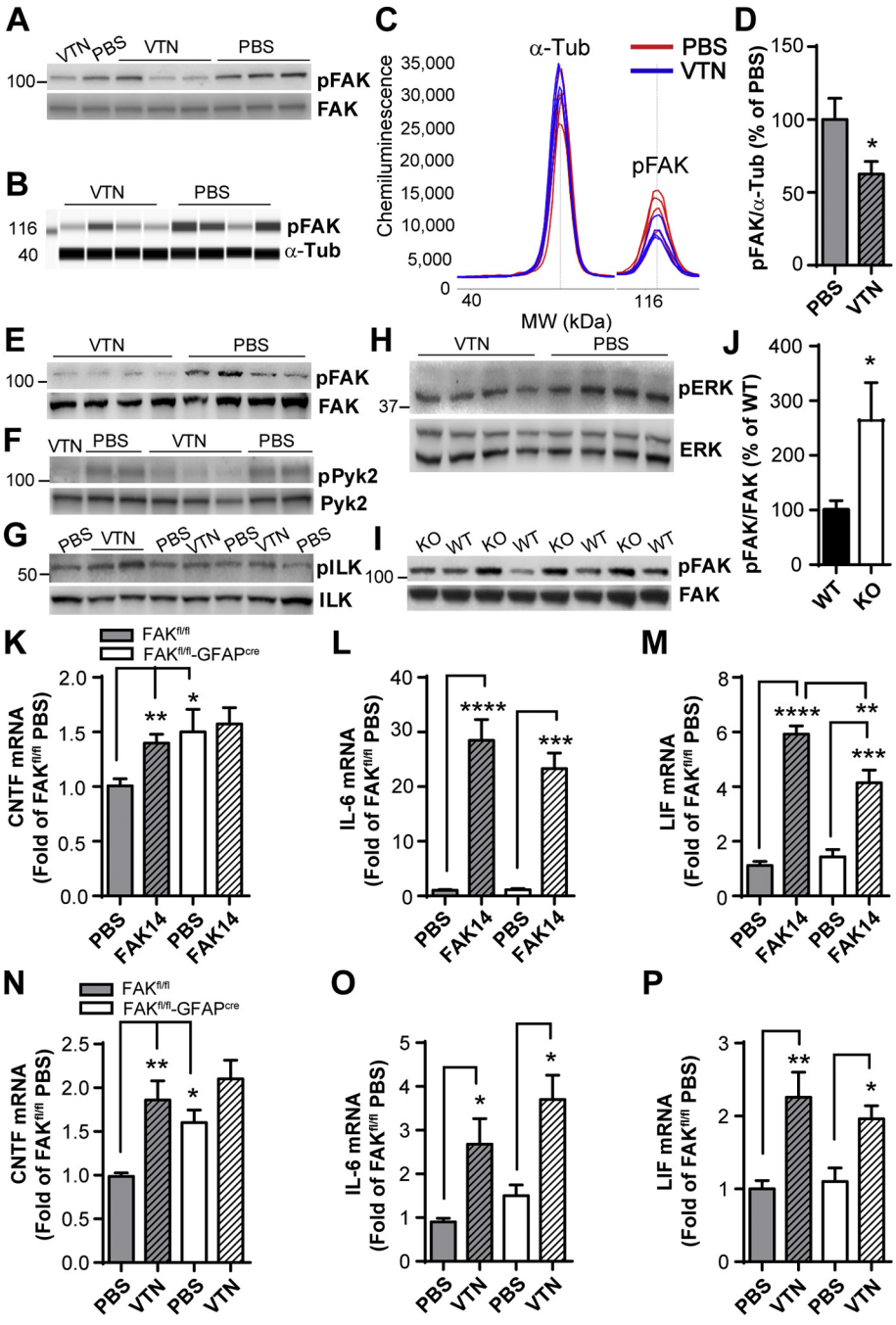

Fig. 6. VTN induces CNTF, IL-6 and LIF expression through FAK inhibition. A) Intrastriatal injection of rhVTN in VTN+/+ wildtype mice reduced pFAK in the SVZ 3 h later as shown by Western blot (Representative of 3 independent blots). B) Quantitative capillary westerns document the decreases in pFAK as shown in synthetic computer-generated bands and by C) chemiluminescence traces of individual mice. D) pFAK/α-tubulin ratios were measured by the areas under curve. Data are mean + SEM, with PBS set at 100% (n = 4 mice/group. *p < 0.05, Student's *t*-test). E) Representative western blot showing that intrastriatal injection of rhVTN also reduced pFAK at 3 h in the SVZ of C57BL/6 mice. Injection of rhVTN decreased pPyk2 (F), increased pILK (G) and reduced pERK (H) in the SVZ of VTN+/+ mice at 3 h. I–J) Representative western blot and densitometry quantification showing that VTN−/− mice have increased pFAK in the SVZ ($n = 7$ and 5 mice, *p < 0.05, Student's *t*-test). Astrocyte-specific genetic deletion of FAK ($FAK^{fl/fl}$-$GFAP^{cre}$ mice) increased mRNA levels of CNTF (K), but not IL-6 (L) or LIF (M) in the SVZ (compare the intrastriatal PBS-injected groups). Intrastriatal injection of FAK inhibitor, FAK14, increased CNTF, IL-6 and LIF mRNA in the SVZ of control $FAK^{fl/fl}$ mice at 24 h. However, FAK14 had no effect on CNTF (K) in the SVZ of $FAK^{fl/fl}$-$GFAP^{cre}$ mice, indicating that it acts via FAK to induce CNTF. FAK14 induced IL-6 to the same extent in control and cre-lox mice (L) and had less effect on LIF in the $FAK^{fl/fl}$-$GFAP^{cre}$ compared to the control mice (M). Data are mean + SEM and calculated as a fold change over $FAK^{fl/fl}$ mice PBS group average (n = 7, 8, 6 and 4 mice/group. *p < 0.05, **p < 0.01, ***p < 0.001, ****p < 0.0001, Two-way ANOVA followed by post hoc Tukey multiple comparison test). N) Intrastriatal injection of rhVTN increased CNTF mRNA in the SVZ of $FAK^{fl/fl}$ but not $FAK^{fl/fl}$-$GFAP^{cre}$ mice at 24 h, indicating that it acts via astroglial FAK to induce CNTF. Intrastriatal injection of rhVTN induced IL-6 O) and LIF P) in both control and cre-lox mice (n = 8, 5, 4 and 5 mice/group. *p < 0.05, **p < 0.01, Two-way ANOVA followed by post hoc Tukey multiple comparison test).

tissues (Leavesley et al., 2013; Preissner and Reuning, 2011) and this study adds important new insight for its normal function in the brain and points to the potential to utilize its activities to regulate cytokine expression and increase neurogenesis. Our data suggest that VTN has rapid actions in the adult brain where SVZ neurogenesis was substantially increased as early as 48 h. This suggests that it has a dynamic function, which is not expected of ECM molecules in the tissue basement membranes, but is consistent with its functions as a soluble molecule, in the same way as it does in blood.

In the forebrain, we detected VTN staining with a validated antibody exclusively in pericytes and their processes around the microvasculature. A recent transcriptome study of normal mouse brain tissue identified VTN as a potential marker for pericytes (He et al., 2016). Others reported VTN mRNA in endothelial cells around blood vessels in the developing mouse brain using radioactive in situ hybridization (Seiffert et al., 1995) but the pattern of staining is consistent with pericytes. We also find that abundant VTN seems to be present in pericytes of the liver (also named stellate cells) and heart. The fibrous pattern of staining in skeletal muscle, lung, kidney and skin shown in the study describing the discovery of VTN (Hayman et al., 1983) is also consistent with pericytes. Our finding that hepatocytes have very little detectable VTN is consistent with previous reports of strong perivascular and sinusoidal VTN staining (Edwards et al., 2006; Kobayashi et al., 1994), but apparently discrepant with the reports that hepatocytes are the main producers of VTN (Kobayashi et al., 1994; Seiffert et al., 1991). Others have suggested that the low abundance of VTN in hepatocytes is due to their rapid release into the blood stream as is also true for other blood proteins such as albumin (Inuzuka et al., 1992; Kobayashi et al., 1994). The relative contribution of hepatocytes and pericytes, and by pericytes of different organs, to blood VTN remains to be determined.

Pericytes are embedded in a common basement membrane with

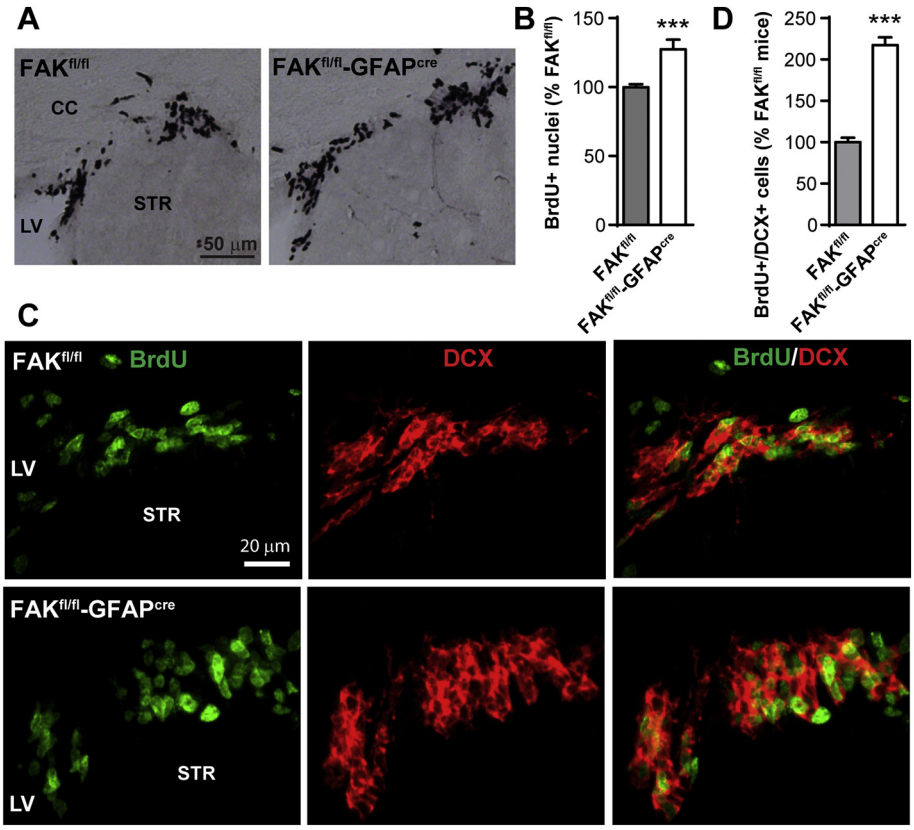

Fig. 7. Astrocyte-specific knockout of FAK increases SVZ neurogenesis. A) Representative images of BrdU immunostaining in coronal sections through the dorsolateral SVZ of adult $FAK^{fl/fl}$ and $FAK^{fl/fl}$-$GFAP^{cre}$ mice following 3 daily BrdU injections show an increase in proliferation in the SVZ of $FAK^{fl/fl}$-$GFAP^{cre}$ mice. B) Unbiased stereological counting of BrdU-positive nuclei in the SVZ confirmed that $FAK^{fl/fl}$-$GFAP^{cre}$ mice had ~27% more cell proliferation than $FAK^{fl/fl}$ mice (n = 9 and 7 mice, ***$p < 0.001$, student's *t*-test). C) Representative images of BrdU (green) and DCX (red) immunostaining in the dorsolateral SVZ of adult $FAK^{fl/fl}$ and $FAK^{fl/fl}$-$GFAP^{cre}$ mice show an increase in neurogenesis in the SVZ of $FAK^{fl/fl}$-$GFAP^{cre}$ mice. LV = lateral ventricle, STR = striatum and CC = corpus callosum. D) Quantification of BrdU-DCX co-labeled cells in the SVZ confirmed that $FAK^{fl/fl}$-$GFAP^{cre}$ mice had ~2 fold more neurogenesis than $FAK^{fl/fl}$ mice (n = 9 and 7 mice, ***$p < 0.001$, student's *t*-test). (For interpretation of the references to colour in this figure legend, the reader is referred to the web version of this article.)

endothelial cells (Dore-Duffy and Cleary, 2011). The brain has the highest pericyte density and microvascular coverage among organs, having up to 3:1 ratios over endothelial cells (Armulik et al., 2011; Frank et al., 1990). Pericytes are uniquely positioned in the neurovascular unit between endothelial cells, glial cells and neurons. They integrate signals from these cells to maintain brain functions in health and disease, including blood-brain barrier permeability, angiogenesis, blood flow regulation and repair (Choi et al., 2016; Sweeney et al., 2016; Trost et al., 2016). Pericytes play a role as inflammatory mediators (Rustenhoven et al., 2017). Our results suggest that their production and release of VTN contribute to these roles. VTN mRNA was abundantly expressed in the adult mouse SVZ (qPCR Ct values of ~22) and protein staining was abundant in a subpopulation of pericytes located at bifurcations of microvessels. This suggests that VTN is constantly produced, which would be consistent with a dynamic function, e.g., as a regulator of gene expression.

The novel role of pericyte VTN in regulating cytokine expression and neurogenesis is consistent with the reported interplay between pericytes and endothelial cells, which regulates SVZ neurogenesis (Crouch et al., 2015), with pericytes releasing diffusible signals in vitro. Brain pericytes release molecules such as TGFβ and BMPs to regulate proliferation and migration of CNS progenitor cells (Choe et al., 2014; Maki et al., 2015). VTN is known to promote endothelial cell survival, probably through αvβ3 integrin (Franco et al., 2011; Isik et al., 1998), and endothelial cells also promote neurogenesis, possibly through VEGF (Sun et al., 2010). We found that VTN-positive pericytes were ensheathed by astrocyte processes. VTN is an adhesion molecule for astrocytes, binding αvβ5 integrin (Gladson et al., 2000). Moreover, astrocytes can translate transcripts in their peripheral processes (Sakers et al., 2017), raising the possibility that pericytes affect astrocyte protein expression locally, in addition to retrograde signaling to their nuclei, in order to regulate neurogenesis. Clearly, there is a special relationship between pericytes, endothelial cells and astrocytes in which VTN could play an important role. It remains to be determined which cell types in the SVZ respond directly to VTN to produce CNTF, LIF and IL-6. Astrocytes and microglia are most likely responders, since both cell types express αvβ3 and/or αvβ5 integrin (Milner, 2009; Herrera-Molina et al., 2012; Tawil et al., 1994). Both cells produce LIF and IL-6, and astrocytes produce CNTF after injury (Kang et al., 2013a; Kang et al., 2012; Keasey et al., 2013; Milner et al., 2007; Van Wagoner and Benveniste, 1999; Van Wagoner et al., 1999; Yang et al., 2008). Our data with inducible conditional FAK knockout mice suggest that VTN induces CNTF expression in the astrocytes, VTN-induced IL-6 is not from astrocytes and VTN-induced LIF regulation may include multiple cell types.

Our results indicate that VTN regulates neurogenesis by inducing pro-neurogenic CNTF as well as LIF and IL-6, which stimulate neural stem cell self-renew at the expense of rapidly proliferating C-cell progenitors and neuroblast formation in the SVZ (Bauer and Patterson, 2006; Bowen et al., 2011; Buono et al., 2012; Covey et al., 2011; Storer et al., 2018). LIF and IL-6 counteract CNTF functions in promoting neurogenesis after stroke (Kang et al., 2013a). The finely tuned balance between stem cell proliferation and neurogenesis can be modified by reducing LIF and IL-6, but not CNTF, expression with the gp130 inhibitor SC144, leading to an increase in progenitor proliferation and neuroblast formation. This is supported by systemic FAK14 injections, which only induces CNTF and increases neurogenesis (Jia et al., unpublished data). These data identify gp130 as a potentially novel therapeutic target to induce neurogenesis, e.g., by combining SC144 with small integrin agonist peptides which mimic VTN. Injection of VTN alone did not change neurogenesis but increased FGF2 in the SVZ, suggesting that LIF and IL-6 act to reduce formation of progenitors that can respond to the increased FGF2. Interestingly, IL-6 can stimulate VTN expression in the liver (Seiffert et al., 1995), raising the possibility that a feedforward mechanism might exist in the SVZ. Perhaps, co-expression of CNTF prevents excessive IL-6 expression, as suggested by our findings in CNTF−/− mice after stroke (Kang et al., unpublished). How the balances of these cytokines change over time and affects

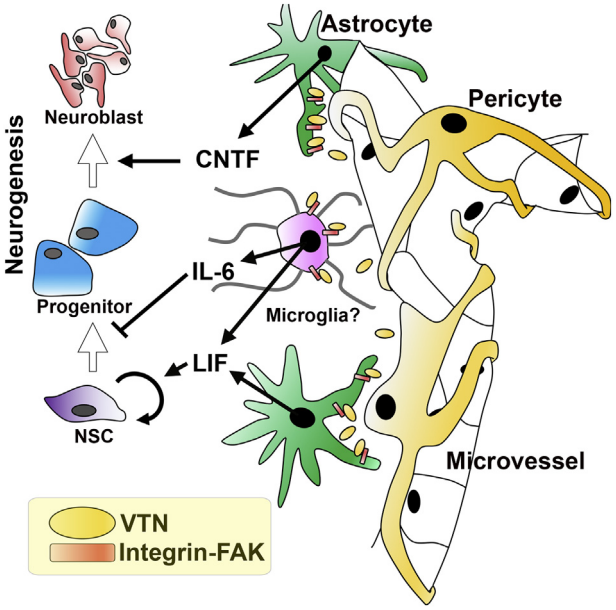

Fig. 8. Summary of VTN-induced SVZ neurogenesis through CNTF. VTN is uniquely expressed in the pericytes located on the abluminal surface of a capillary. Released VTN binds integrins on the astrocytes which leads to FAK inhibition and subsequent CNTF induction which promotes neurogenesis in the SVZ. LIF is increased in part through FAK inhibition in astrocytes and IL-6 is produced by another cell type, possibly microglia. CNTF promotes neurogenesis, while LIF and IL-6 inhibits neurogenesis by promoting neural stem cell self-renewal and/or inhibiting production of neural progenitor cells.

individual cells are unclear, but most likely involves many additional molecular regulators of stem cells, progenitors and neuroblasts. All these cells are needed to enable production of new neurons throughout life.

LIF and IL-6 are expressed at very low levels in the brain under physiological conditions and rapidly increase upon injuries (Kang et al., 2013a; Quintana et al., 2008; Sriram et al., 2004). The mechanisms that regulate these cytokines under naïve and injury conditions are unclear but our results suggest that they include VTN. The finding that gp130 regulates VTN-induced LIF and IL-6, but not CNTF, expression is unexpected because CNTF can be regulated by the gp130-JAK-STAT pathway (Ip et al., 1992). The gp130 ligand IL-6 stimulates p705 STAT3 (Keasey et al., 2013), which binds to the CNTF promoter (Keasey et al., 2013), and stimulates CNTF expression (Kang et al., 2012; Shuto et al., 2001). It is possible that this apparent discrepancy is caused by additional VTN signaling properties, e.g., through its binding to uPAR (Ferraris et al., 2014; Madsen et al., 2007). Collectively, our data reveal a surprising differential regulation mechanisms of these closely related cytokines by VTN, and may provide opportunities to individually regulate them. It remains to be determined whether VTN also regulates hippocampal neurogenesis through these pathways and whether they contribute to age- and disease-related changes in neurogenesis.

Integrin-binding ECM molecules like VTN activate FAK through phosphorylation in vitro (Hecker et al., 2004). Here, intracerebral VTN injections caused a reduction in pFAK and the closely related PYK2 at 3 h, while activating ILK. Moreover, the SVZ of VTN−/− mice had higher levels of pFAK compared to VTN+/+ mice. Also, intracerebral injection of FAK inhibitor caused the same increase in cytokine expression as did VTN injections, and increased CNTF and LIF through astroglial FAK as shown in the GFAP-cre-FAK-lox mice. Future studies will have to determine the mechanisms underlying this unexpected finding. It is possible that the acutely reduced ERK phosphorylation we observed (Fig. 7H) resulted in a subsequent reduction of ERK-dependent FAK phosphorylation (Zheng et al., 2009), as a feedback mechanism. The VTN effects may be cell context-dependent as is seen with EGF, which can rapidly suppress phosphorylation of FAK Y397 in cultured keratinocytes with high pFAK but stimulates it in those with low pFAK (Kim and Kim, 2008). Our finding that VTN had the opposite effects on pILK than pFAK has also been described for another integrin ligand, osteopontin (Li et al., 2007).

5. Conclusion

These data identify a novel role of VTN uniquely produced by brain pericytes on cytokine expression and neurogenesis in the SVZ (Fig. 8). VTN induces co-expression of pro-neurogenic CNTF, and LIF and IL-6, known to promote neural stem cell renewal and inhibit progenitor formation. Importantly, pharmacological inhibition of the IL-6-gp130 receptor, dampened VTN-induced LIF and IL-6, but not CNTF expression, and rapidly increased neurogenesis. Also, VTN induces these cytokines through inhibiting FAK and specific FAK inhibition in astrocytes promotes CNTF expression. This study identifies potentially new therapeutic targets to promote neurogenesis for cell replacement in the brain.

Acknowledgements

We appreciated Dr. Diego Rodriguez-Gil who provided the Ai6 breeder mice. We express our gratitude to Aruna Visavadiya, Jacob Elam, the Molecular Core Facility and Microscopy Core Facility for technical support, and Dr. Paul Monaco for his advice on liver and heart histology.

Author contributions

C.J. and T.H. designed research, C.J., H.M., C.L., R.S. and V.R. performed the experiments, C.J. and T.H. analyzed the data, and C.J., M.P.K. and T.H. interpreted the data and wrote the paper.

Funding sources

This work was supported by NIH grant AG029493 and in part by NIH grant C06RR0306551 and funds from the Quillen College of Medicine at East Tennessee State University.

Conflict of interest

The authors declare no competing financial interests.

Appendix A. Supplementary data

Supplementary data to this article can be found online at https://doi.org/10.1016/j.expneurol.2018.11.002.

References

Aberg, M.A., Aberg, N.D., Palmer, T.D., Alborn, A.M., Carlsson-Skwirut, C., Bang, P., Rosengren, L.E., Olsson, T., Gage, F.H., Eriksson, P.S., 2003. IGF-I has a direct proliferative effect in adult hippocampal progenitor cells. Mol. Cell. Neurosci. 24, 23–40.
Acevedo, L.M., Lindquist, J.N., Walsh, B.M., Sia, P., Cimadamore, F., Chen, C., Denzel, M., Pernia, C.D., Ranscht, B., Terskikh, A., Snyder, E.Y., Cheresh, D.A., 2015. hESC differentiation toward an autonomic neuronal cell fate depends on distinct cues from the co-patterning vasculature. Stem Cell Rep. 4, 1075–1088.
Alvarez-Buylla, A., Lim, D.A., 2004. For the long run: maintaining germinal niches in the adult brain. Neuron 41, 683–686.
Armulik, A., Genove, G., Betsholtz, C., 2011. Pericytes: developmental, physiological, and pathological perspectives, problems, and promises. Dev. Cell 21, 193–215.
Bae, H.B., Zmijewski, J.W., Deshane, J.S., Zhi, D., Thompson, L.C., Peterson, C.B., Chaplin, D.D., Abraham, E., 2012. Vitronectin inhibits neutrophil apoptosis through activation of integrin-associated signaling pathways. Am. J. Respir. Cell Mol. Biol. 46, 790–796.
Bauer, S., Patterson, P.H., 2006. Leukemia inhibitory factor promotes neural stem cell self-renewal in the adult brain. J. Neurosci. 26, 12089–12099.
Bello, L., Francolini, M., Marthyn, P., Zhang, J., Carroll, R.S., Nikas, D.C., Strasser, J.F., Villani, R., Cheresh, D.A., Black, P.M., 2001. Alpha(v)beta3 and alpha(v)beta5

integrin expression in glioma periphery. Neurosurgery 49, 380–389 (discussion 390).
Bergmann, S., Lang, A., Rohde, M., Agarwal, V., Rennemeier, C., Grashoff, C., Preissner, K.T., Hammerschmidt, S., 2009. Integrin-linked kinase is required for vitronectin-mediated internalization of Streptococcus pneumoniae by host cells. J. Cell Sci. 122, 256–267.
Bowen, K.K., Dempsey, R.J., Vemuganti, R., 2011. Adult interleukin-6 knockout mice show compromised neurogenesis. Neuroreport 22, 126–130.
Buono, K.D., Vadlamuri, D., Gan, Q., Levison, S.W., 2012. Leukemia inhibitory factor is essential for subventricular zone neural stem cell and progenitor homeostasis as revealed by a novel flow cytometric analysis. Dev. Neurosci. 34, 449–462.
Choe, Y., Huynh, T., Pleasure, S.J., 2014. Migration of oligodendrocyte progenitor cells is controlled by transforming growth factor beta family proteins during corticogenesis. J. Neurosci. 34, 14973–14983.
Choi, Y.K., Maki, T., Mandeville, E.T., Koh, S.H., Hayakawa, K., Arai, K., Kim, Y.M., Whalen, M.J., Xing, C., Wang, X., Kim, K.W., Lo, E.H., 2016. Dual effects of carbon monoxide on pericytes and neurogenesis in traumatic brain injury. Nat. Med. 22, 1335–1341.
Covey, M.V., Loporchio, D., Buono, K.D., Levison, S.W., 2011. Opposite effect of inflammation on subventricular zone versus hippocampal precursors in brain injury. Ann. Neurol. 70, 616–626.
Crouch, E.E., Liu, C., Silva-Vargas, V., Doetsch, F., 2015. Regional and stage-specific effects of prospectively purified vascular cells on the adult V-SVZ neural stem cell lineage. J. Neurosci. 35, 4528–4539.
Delgado, A.C., Ferron, S.R., Vicente, D., Porlan, E., Perez-Villalba, A., Trujillo, C.M., D'Ocon, P., Farinas, I., 2014. Endothelial NT-3 delivered by vasculature and CSF promotes quiescence of subependymal neural stem cells through nitric oxide induction. Neuron 83, 572–585.
Di Matteo, P., Arrigoni, G.L., Alberici, L., Corti, A., Gallo-Stampino, C., Traversari, C., Doglioni, C., Rizzardi, G.P., 2011. Enhanced expression of CD13 in vessels of inflammatory and neoplastic tissues. J. Histochem. Cytochem. 59, 47–59.
Doetsch, F., Caille, I., Lim, D.A., Garcia-Verdugo, J.M., Alvarez-Buylla, A., 1999. Subventricular zone astrocytes are neural stem cells in the adult mammalian brain. Cell 97, 703–716.
Doetsch, F., Verdugo, J.M., Caille, I., Alvarez-Buylla, A., Chao, M.V., Casaccia-Bonnefil, P., 2002. Lack of the cell-cycle inhibitor p27Kip1 results in selective increase of transit-amplifying cells for adult neurogenesis. J. Neurosci. 22, 2255–2264.
Dore-Duffy, P., Cleary, K., 2011. Morphology and properties of pericytes. Methods Mol. Biol. 686, 49–68.
Douet, V., Arikawa-Hirasawa, E., Mercier, F., 2012. Fractone-heparan sulfates mediate BMP-7 inhibition of cell proliferation in the adult subventricular zone. Neurosci. Lett. 528, 120–125.
Dufourcq, P., Couffinhal, T., Alzieu, P., Daret, D., Moreau, C., Duplaa, C., Bonnet, J., 2002. Vitronectin is up-regulated after vascular injury and vitronectin blockade prevents neointima formation. Cardiovasc. Res. 53, 952–962.
Eberhard, T., Ullberg, M., 2002. Interaction of vitronectin with Haemophilus influenzae. FEMS Immunol. Med. Microbiol. 34, 215–219.
Edwards, S., Lalor, P.F., Tuncer, C., Adams, D.H., 2006. Vitronectin in human hepatic tumours contributes to the recruitment of lymphocytes in an alpha v beta3-independent manner. Br. J. Cancer 95, 1545–1554.
Eitzman, D.T., Westrick, R.J., Nabel, E.G., Ginsburg, D., 2000. Plasminogen activator inhibitor-1 and vitronectin promote vascular thrombosis in mice. Blood 95, 577–580.
Emanueli, C., Schratzberger, P., Kirchmair, R., Madeddu, P., 2003. Paracrine control of vascularization and neurogenesis by neurotrophins. Br. J. Pharmacol. 140, 614–619.
Emsley, J.G., Hagg, T., 2003a. alpha6beta1 integrin directs migration of neuronal precursors in adult mouse forebrain. Exp. Neurol. 183, 273–285.
Emsley, J.G., Hagg, T., 2003b. Endogenous and exogenous ciliary neurotrophic factor enhances forebrain neurogenesis in adult mice. Exp. Neurol. 183, 298–310.
Ernst, A., Alkass, K., Bernard, S., Salehpour, M., Perl, S., Tisdale, J., Possnert, G., Druid, H., Frisen, J., 2014. Neurogenesis in the striatum of the adult human brain. Cell 156, 1072–1083.
Ferraris, G.M., Schulte, C., Buttiglione, V., De Lorenzi, V., Piontini, A., Galluzzi, M., Podesta, A., Madsen, C.D., Sidenius, N., 2014. The interaction between uPAR and vitronectin triggers ligand-independent adhesion signalling by integrins. EMBO J. 33, 2458–2472.
Franco, M., Roswall, P., Cortez, E., Hanahan, D., Pietras, K., 2011. Pericytes promote endothelial cell survival through induction of autocrine VEGF-A signaling and Bcl-w expression. Blood 118, 2906–2917.
Frank, R.N., Turczyn, T.J., Das, A., 1990. Pericyte coverage of retinal and cerebral capillaries. Invest. Ophthalmol. Vis. Sci. 31, 999–1007.
Giancotti, F.G., Ruoslahti, E., 1999. Integrin signaling. Science 285, 1028–1032.
Gladson, C.L., Stewart, J.E., Olman, M.A., Chang, P.L., Schnapp, L.M., Grammer, J.R., Benveniste, E.N., 2000. Attachment of primary neonatal rat astrocytes to vitronectin is mediated by integrins alphavbeta5 and alpha8beta1: modulation by the type 1 plasminogen activator inhibitor. Neurosci. Lett. 283, 157–161.
Grande, F., Aiello, F., Garofalo, A., Neamati, N., 2016. Identification and preclinical evaluation of SC144, a novel pyrroloquinoxaline derivative with broad-spectrum anticancer activity. Mini Rev. Med. Chem. 16, 644–650.
Gregg, C., Weiss, S., 2005. CNTF/LIF/gp130 receptor complex signaling maintains a VZ precursor differentiation gradient in the developing ventral forebrain. Development 132, 565–578.
Hagg, T., 2009. From neurotransmitters to neurotrophic factors to neurogenesis. Neuroscientist 15, 20–27.
Hall, C.N., Reynell, C., Gesslein, B., Hamilton, N.B., Mishra, A., Sutherland, B.A., O'Farrell, F.M., Buchan, A.M., Lauritzen, M., Attwell, D., 2014. Capillary pericytes regulate cerebral blood flow in health and disease. Nature 508, 55–60.
Hallstrom, T., Trajkovska, E., Forsgren, A., Riesbeck, K., 2006. Haemophilus influenzae surface fibrils contribute to serum resistance by interacting with vitronectin. J. Immunol. 177, 430–436.
Harris, G.M., Madigan, N.N., Lancaster, K.Z., Enquist, L.W., Windebank, A.J., Schwartz, J., Schwarzbauer, J.E., 2017. Nerve guidance by a decellularized fibroblast extracellular matrix. Matrix Biol. 60-61, 176–189.
Hashimoto, K., Sakane, F., Ikeda, N., Akiyama, A., Sugahara, M., Miyamoto, Y., 2016. Vitronectin promotes the progress of the initial differentiation stage in cerebellar granule cells. Mol. Cell. Neurosci. 70, 76–85.
Hayman, E.G., Pierschbacher, M.D., Ohgren, Y., Ruoslahti, E., 1983. Serum spreading factor (vitronectin) is present at the cell surface and in tissues. Proc. Natl. Acad. Sci. U. S. A. 80, 4003–4007.
He, L., Vanlandewijck, M., Raschperger, E., Andaloussi Mae, M., Jung, B., Lebouvier, T., Ando, K., Hofmann, J., Keller, A., Betsholtz, C., 2016. Analysis of the brain mural cell transcriptome. Sci. Rep. 6, 35108.
Hecker, T.P., Ding, Q., Rege, T.A., Hanks, S.K., Gladson, C.L., 2004. Overexpression of FAK promotes Ras activity through the formation of a FAK/p120RasGAP complex in malignant astrocytoma cells. Oncogene 23, 3962–3971.
Hellerbrand, C., 2013. Hepatic stellate cells–the pericytes in the liver. Pflugers Arch. 465, 775–778.
Herrera-Molina, R., Frischknecht, R., Maldonado, H., Seidenbecher, C.I., Gundelfinger, E.D., Hetz, C., Aylwin Mde, L., Schneider, P., Quest, A.F., Leyton, L., 2012. Astrocytic alphaVbeta3 integrin inhibits neurite outgrowth and promotes retraction of neuronal processes by clustering Thy-1. PLoS One 7, e34295.
Hogasen, K., Mollnes, T.E., Tschopp, J., Harboe, M., 1993. Quantitation of vitronectin and clusterin. Pitfalls and solutions in enzyme immunoassays for adhesive proteins. J. Immunol. Methods 160, 107–115.
Huang, R., Pan, Q., Ma, X., Wang, Y., Liang, Y., Dai, B., Liao, X., Li, M., Miao, H., 2016. Hepatic stellate cell-derived microvesicles prevent hepatocytes from injury induced by APAP/H2O2. Stem Cells Int. 2016, 8357567.
Hunter, T., Eckhart, W., 2004. The discovery of tyrosine phosphorylation: it's all in the buffer!. Cell 116, S35–39 31 (P following S48).
Inuzuka, S., Ueno, T., Torimura, T., Tamaki, S., Sakata, R., Sata, M., Yoshida, H., Tanikawa, K., 1992. Vitronectin in liver disorders: biochemical and immunohistochemical studies. Hepatology 15, 629–636.
Ip, N.Y., Boulton, T.G., Li, Y., Verdi, J.M., Birren, S.J., Anderson, D.J., Yancopoulos, G.D., 1994. CNTF, FGF, and NGF collaborate to drive the terminal differentiation of MAH cells into postmitotic neurons. Neuron 13, 443–455.
Ip, N.Y., Nye, S.H., Boulton, T.G., Davis, S., Taga, T., Li, Y., Birren, S.J., Yasukawa, K., Kishimoto, T., Anderson, D.J., et al., 1992. CNTF and LIF act on neuronal cells via shared signaling pathways that involve the IL-6 signal transducing receptor component gp130. Cell 69, 1121–1132.
Isik, F.F., Gibran, N.S., Jang, Y.C., Sandell, L., Schwartz, S.M., 1998. Vitronectin decreases microvascular endothelial cell apoptosis. J. Cell. Physiol. 175, 149–155.
Jang, Y.C., Tsou, R., Gibran, N.S., Isik, F.F., 2000. Vitronectin deficiency is associated with increased wound fibrinolysis and decreased microvascular angiogenesis in mice. Surgery 127, 696–704.
Jia, C., Hegg, C.C., 2015. Effect of IP3R3 and NPY on age-related declines in olfactory stem cell proliferation. Neurobiol. Aging 36, 1045–1056.
Jia, C., Keasey, M.P., Lovins, C., Hagg, T., 2018. Inhibition of astrocyte FAK-JNK signaling promotes subventricular zone neurogenesis through CNTF. Glia (In press).
Kang, S.S., Keasey, M.P., Arnold, S.A., Reid, R., Geralds, J., Hagg, T., 2013a. Endogenous CNTF mediates stroke-induced adult CNS neurogenesis in mice. Neurobiol. Dis. 49, 68–78.
Kang, S.S., Keasey, M.P., Cai, J., Hagg, T., 2012. Loss of neuron-astroglial interaction rapidly induces protective CNTF expression after stroke in mice. J. Neurosci. 32, 9277–9287.
Kang, S.S., Keasey, M.P., Hagg, T., 2013b. P2X7 receptor inhibition increases CNTF in the subventricular zone, but not neurogenesis or neuroprotection after stroke in adult mice. Transl Stroke Res 4, 533–545.
Keasey, M.P., Jia, C., Pimentel, L.F., Sante, R.R., Lovins, C., Hagg, T., 2018. Blood vitronectin is a major activator of LIF and IL-6 in the brain through integrin-FAK and uPAR signaling. J. Cell Sci. 131.
Keasey, M.P., Kang, S.S., Lovins, C., Hagg, T., 2013. Inhibition of a novel specific neuroglial integrin signaling pathway increases STAT3-mediated CNTF expression. Cell Commun. Signal 11, 35.
Kim, S.H., Kim, S.H., 2008. Antagonistic effect of EGF on FAK phosphorylation/dephosphorylation in a cell. Cell Biochem. Funct. 26, 539–547.
Kitchens, D.L., Snyder, E.Y., Gottlieb, D.I., 1994. FGF and EGF are mitogens for immortalized neural progenitors. J. Neurobiol. 25, 797–807.
Kobayashi, J., Yamada, S., Kawasaki, H., 1994. Distribution of vitronectin in plasma and liver tissue: relationship to chronic liver disease. Hepatology 20, 1412–1417.
Kuhn, H.G., Winkler, J., Kempermann, G., Thal, L.J., Gage, F.H., 1997. Epidermal growth factor and fibroblast growth factor-2 have different effects on neural progenitors in the adult rat brain. J. Neurosci. 17, 5820–5829.
Leavesley, D.I., Kashyap, A.S., Croll, T., Sivaramakrishnan, M., Shokoohmand, A., Hollier, B.G., Upton, Z., 2013. Vitronectin–master controller or micromanager? IUBMB Life 65, 807–818.
Li, X., Barkho, B.Z., Luo, Y., Smrt, R.D., Santistevan, N.J., Liu, C., Kuwabara, T., Gage, F.H., Zhao, X., 2008. Epigenetic regulation of the stem cell mitogen Fgf-2 by Mbd1 in adult neural stem/progenitor cells. J. Biol. Chem. 283, 27644–27652.
Li, J.J., Han, M., Wen, J.K., Li, A.Y., 2007. Osteopontin stimulates vascular smooth muscle cell migration by inducing FAK phosphorylation and ILK dephosphorylation. Biochem. Biophys. Res. Commun. 356, 13–19.
Lin, R., Lang, M., Heinsinger, N., Stricsek, G., Zhang, J., Iozzo, R., Rosenwasser, R., Iacovitti, L., 2018. Stepwise impairment of neural stem cell proliferation and neurogenesis concomitant with disruption of blood-brain barrier in recurrent ischemic

stroke. Neurobiol. Dis. 115, 49–58.
Liu, S., Agalliu, D., Yu, C., Fisher, M., 2012. The role of pericytes in blood-brain barrier function and stroke. Curr. Pharm. Des. 18, 3653–3662.
Madsen, C.D., Ferraris, G.M., Andolfo, A., Cunningham, O., Sidenius, N., 2007. uPAR-induced cell adhesion and migration: vitronectin provides the key. J. Cell Biol. 177, 927–939.
Maki, T., Maeda, M., Uemura, M., Lo, E.K., Terasaki, Y., Liang, A.C., Shindo, A., Choi, Y.K., Taguchi, A., Matsuyama, T., Takahashi, R., Ihara, M., Arai, K., 2015. Potential interactions between pericytes and oligodendrocyte precursor cells in perivascular regions of cerebral white matter. Neurosci. Lett. 597, 164–169.
Mercier, F., Kitasako, J.T., Hatton, G.I., 2002. Anatomy of the brain neurogenic zones revisited: fractones and the fibroblast/macrophage network. J. Comp. Neurol. 451, 170–188.
Milner, R., Crocker, S.J., Hung, S., Wang, X., Frausto, R.F., del Zoppo, G.J., 2007. Fibronectin- and vitronectin-induced microglial activation and matrix metalloproteinase-9 expression is mediated by integrins alpha5beta1 and alphavbeta5. J. Immunol. 178, 8158–8167.
Milner, R., 2009. Microglial expression of alphavbeta3 and alphavbeta5 integrins is regulated by cytokines and the extracellular matrix: beta5 integrin null microglia show no defects in adhesion or MMP-9 expression on vitronectin. Glia 57, 714–723.
Ming, G.L., Song, H., 2011. Adult neurogenesis in the mammalian brain: significant answers and significant questions. Neuron 70, 687–702.
Mitra, S.K., Hanson, D.A., Schlaepfer, D.D., 2005. Focal adhesion kinase: in command and control of cell motility. Nat. Rev. Mol. Cell Biol. 6, 56–68.
Pasternak, A.O., Adema, K.W., Bakker, M., Jurriaans, S., Berkhout, B., Cornelissen, M., Lukashov, V.V., 2008. Highly sensitive methods based on seminested real-time reverse transcription-PCR for quantitation of human immunodeficiency virus type 1 unspliced and multiply spliced RNA and proviral DNA. J. Clin. Microbiol. 46, 2206–2211.
Pitman, M., Emery, B., Binder, M., Wang, S., Butzkueven, H., Kilpatrick, T.J., 2004. LIF receptor signaling modulates neural stem cell renewal. Mol. Cell. Neurosci. 27, 255–266.
Ponti, G., Obernier, K., Alvarez-Buylla, A., 2013a. Lineage progression from stem cells to new neurons in the adult brain ventricular-subventricular zone. Cell Cycle 12, 1649–1650.
Ponti, G., Obernier, K., Guinto, C., Jose, L., Bonfanti, L., Alvarez-Buylla, A., 2013b. Cell cycle and lineage progression of neural progenitors in the ventricular-subventricular zones of adult mice. Proc. Natl. Acad. Sci. U. S. A. 110, E1045–E1054.
Preissner, K.T., Reuning, U., 2011. Vitronectin in vascular context: facets of a multitalented matricellular protein. Semin. Thromb. Hemost. 37, 408–424.
Preissner, K.T., Seiffert, D., 1998. Role of vitronectin and its receptors in haemostasis and vascular remodeling. Thromb. Res. 89, 1–21.
Quintana, A., Molinero, A., Borup, R., Nielsen, F.C., Campbell, I.L., Penkowa, M., Hidalgo, J., 2008. Effect of astrocyte-targeted production of IL-6 on traumatic brain injury and its impact on the cortical transcriptome. Dev. Neurobiol. 68, 195–208.
Rustenhoven, J., Jansson, D., Smyth, L.C., Dragunow, M., 2017. Brain Pericytes as Mediators of Neuroinflammation. Trends Pharmacol. Sci. 38, 291–304.
Sakers, K., Lake, A.M., Khazanchi, R., Ouwenga, R., Vasek, M.J., Dani, A., Dougherty, J.D., 2017. Astrocytes locally translate transcripts in their peripheral processes. Proc. Natl. Acad. Sci. U. S. A. 114 (E3830-E3838).
Sato, H., Ishii, Y., Yamamoto, S., Azuma, E., Takahashi, Y., Hamashima, T., Umezawa, A., Mori, H., Kuroda, S., Endo, S., Sasahara, M., 2016. PDGFR-beta plays a key role in the ectopic migration of neuroblasts in cerebral stroke. Stem Cells 34, 685–698.
Seiffert, D., Bordin, G.M., Loskutoff, D.J., 1996. Evidence that extrahepatic cells express vitronectin mRNA at rates approaching those of hepatocytes. Histochem. Cell Biol. 105, 195–201.
Seiffert, D., Geisterfer, M., Gauldie, J., Young, E., Podor, T.J., 1995. IL-6 stimulates vitronectin gene expression in vivo. J. Immunol. 155, 3180–3185.
Seiffert, D., Iruela-Arispe, M.L., Sage, E.H., Loskutoff, D.J., 1995. Distribution of vitronectin mRNA during murine development. Dev. Dyn. 203, 71–79.
Seiffert, D., Keeton, M., Eguchi, Y., Sawdey, M., Loskutoff, D.J., 1991. Detection of vitronectin mRNA in tissues and cells of the mouse. Proc. Natl. Acad. Sci. U. S. A. 88, 9402–9406.
Shaffer, M.C., Foley, T.P., Barnes, D.W., 1984. Quantitation of spreading factor in human biologic fluids. J. Lab. Clin. Med. 103, 783–791.
Shen, Q., Wang, Y., Kokovay, E., Lin, G., Chuang, S.M., Goderie, S.K., Roysam, B., Temple, S., 2008. Adult SVZ stem cells lie in a vascular niche: a quantitative analysis of niche cell-cell interactions. Cell Stem Cell 3, 289–300.
Shimazaki, T., Shingo, T., Weiss, S., 2001. The ciliary neurotrophic factor/leukemia inhibitory factor/gp130 receptor complex operates in the maintenance of mammalian forebrain neural stem cells. J. Neurosci. 21, 7642–7653.
Shuto, T., Horie, H., Hikawa, N., Sango, K., Tokashiki, A., Murata, H., Yamamoto, I., Ishikawa, Y., 2001. IL-6 up-regulates CNTF mRNA expression and enhances neurite regeneration. Neuroreport 12, 1081–1085.
Soleman, S., Filippov, M.A., Dityatev, A., Fawcett, J.W., 2013. Targeting the neural extracellular matrix in neurological disorders. Neuroscience 253, 194–213.
Sriram, K., Benkovic, S.A., Hebert, M.A., Miller, D.B., O'Callaghan, J.P., 2004. Induction of gp130-related cytokines and activation of JAK2/STAT3 pathway in astrocytes precedes up-regulation of glial fibrillary acidic protein in the 1-methyl-4-phenyl-1,2,3,6-tetrahydropyridine model of neurodegeneration: key signaling pathway for astrogliosis in vivo? J. Biol. Chem. 279, 19936–19947.
Staquicini, F.I., Dias-Neto, E., Li, J., Snyder, E.Y., Sidman, R.L., Pasqualini, R., Arap, W., 2009. Discovery of a functional protein complex of netrin-4, laminin gamma1 chain, and integrin alpha6beta1 in mouse neural stem cells. Proc. Natl. Acad. Sci. U. S. A. 106, 2903–2908.
Storer, M.A., Gallagher, D., Fatt, M.P., Simonetta, J.V., Kaplan, D.R., Miller, F.D., 2018. Interleukin-6 regulates adult neural stem cell numbers during normal and abnormal post-natal development. Stem Cell Rep. 10, 1464–1480.
Sulzmaier, F.J., Jean, C., Schlaepfer, D.D., 2014. FAK in cancer: mechanistic findings and clinical applications. Nat. Rev. Cancer 14, 598–610.
Sun, J., Zhou, W., Ma, D., Yang, Y., 2010. Endothelial cells promote neural stem cell proliferation and differentiation associated with VEGF activated Notch and Pten signaling. Dev. Dyn. 239, 2345–2353.
Sweeney, M.D., Ayyadurai, S., Zlokovic, B.V., 2016. Pericytes of the neurovascular unit: key functions and signaling pathways. Nat. Neurosci. 19, 771–783.
Tawil, N.J., Wilson, P., Carbonetto, S., 1994. Expression and distribution of functional integrins in rat CNS glia. J. Neurosci. Res. 39, 436–447.
Tavazoie, M., Van der Veken, L., Silva-Vargas, V., Louissaint, M., Colonna, L., Zaidi, B., Garcia-Verdugo, J.M., Doetsch, F., 2008. A specialized vascular niche for adult neural stem cells. Cell Stem Cell 3, 279–288.
Tomasini, B.R., Mosher, D.F., 1991. Vitronectin. Prog. Hemost. Thromb. 10, 269–305.
Trost, A., Lange, S., Schroedl, F., Bruckner, D., Motloch, K.A., Bogner, B., Kaser-Eichberger, A., Strohmaier, C., Runge, C., Aigner, L., Rivera, F.J., Reitsamer, H.A., 2016. Brain and retinal pericytes: origin, function and role. Front. Cell. Neurosci. 10, 20.
van Aken, B.E., Seiffert, D., Thinnes, T., Loskutoff, D.J., 1997. Localization of vitronectin in the normal and atherosclerotic human vessel wall. Histochem. Cell Biol. 107, 313–320.
Van Wagoner, N.J., Benveniste, E.N., 1999. Interleukin-6 expression and regulation in astrocytes. J. Neuroimmunol. 100, 124–139.
Van Wagoner, N.J., Oh, J.W., Repovic, P., Benveniste, E.N., 1999. Interleukin-6 (IL-6) production by astrocytes: autocrine regulation by IL-6 and the soluble IL-6 receptor. J. Neurosci. 19, 5236–5244.
Visavadiya, N.P., Keasey, M.P., Razskazovskiy, V., Banerjee, K., Jia, C., Lovins, C., Wright, G.L., Hagg, T., 2016. Integrin-FAK signaling rapidly and potently promotes mitochondrial function through STAT3. Cell Commun. Signal 14, 32.
Wei, Y., Waltz, D.A., Rao, N., Drummond, R.J., Rosenberg, S., Chapman, H.A., 1994. Identification of the urokinase receptor as an adhesion receptor for vitronectin. J. Biol. Chem. 269, 32380–32388.
Widmaier, M., Rognoni, E., Radovanac, K., Azimifar, S.B., Fassler, R., 2012. Integrin-linked kinase at a glance. J. Cell Sci. 125, 1839–1843.
Winkler, E.A., Bell, R.D., Zlokovic, B.V., 2011. Central nervous system pericytes in health and disease. Nat. Neurosci. 14, 1398–1405.
Xu, S., Grande, F., Garofalo, A., Neamati, N., 2013. Discovery of a novel orally active small-molecule gp130 inhibitor for the treatment of ovarian cancer. Mol. Cancer Ther. 12, 937–949.
Xu, S., Oshima, T., Imada, T., Masuda, M., Debnath, B., Grande, F., Garofalo, A., Neamati, N., 2013. Stabilization of MDA-7/IL-24 for colon cancer therapy. Cancer Lett. 335, 421–430.
Yang, P., Arnold, S.A., Habas, A., Hetman, M., Hagg, T., 2008. Ciliary neurotrophic factor mediates dopamine D2 receptor-induced CNS neurogenesis in adult mice. J. Neurosci. 28, 2231–2241.
Zheng, Y., Xia, Y., Hawke, D., Halle, M., Tremblay, M.L., Gao, X., Zhou, X.Z., Aldape, K., Cobb, M.H., Xie, K., He, J., Lu, Z., 2009. FAK phosphorylation by ERK primes Ras-induced tyrosine dephosphorylation of FAK mediated by PIN1 and PTP-PEST. Mol. Cell 35, 11–25.
Zhou, A., Huntington, J.A., Pannu, N.S., Carrell, R.W., Read, R.J., 2003. How vitronectin binds PAI-1 to modulate fibrinolysis and cell migration. Nat. Struct. Biol. 10, 541–544.
Zigmond, R.E., 2011. gp130 cytokines are positive signals triggering changes in gene expression and axon outgrowth in peripheral neurons following injury. Front. Mol. Neurosci. 4, 62.
Zigmond, R.E., 2012. Cytokines that promote nerve regeneration. Exp. Neurol. 238, 101–106.